Atmos. Chem. Phys. Discuss., 6, 8553–8604, 2006
www.atmos-chem-phys-discuss.net/6/8553/2006/

Atmospheric Chemistry and Physics Discussions

Multi-model simulations of the impact of international shipping on atmospheric chemistry and climate in 2000 and 2030

V. Eyring[1], D. S. Stevenson[2], A. Lauer[1], F. J. Dentener[3], T. Butler[4], W. J. Collins[5], K. Ellingsen[6], M. Gauss[6], D. A. Hauglustaine[7], I. S. A. Isaksen[6], M. G. Lawrence[4], A. Richter[8], J. M. Rodriguez[9], M. Sanderson[5], S. E. Strahan[9], K. Sudo[10], S. Szopa[7], T. P. C. van Noije[11], and O. Wild[10,*]

[1]DLR, Institut für Physik der Atmosphäre, Oberpfaffenhofen, Germany
[2]University of Edinburgh, School of GeoSciences, Edinburgh, United Kingdom
[3]European Commission, Joint Research Centre, Institute for Environment and Sustainability, Ispra, Italy
[4]Max Planck Institute for Chemistry, Mainz, Germany
[5]Met Office, Exeter, United Kingdom
[6]University of Oslo, Department of Geosciences, Oslo, Norway
[7]Laboratoire des Sciences du Climat et de l'Environnement, Gif-sur-Yvette, France
[8]University of Bremen, Institute for Environmental Physics, Bremen, Germany

[9]Goddard Earth Science & Technology Center (GEST), Maryland, Washington, DC, USA
[10]Frontier Research Center for Global Change, JAMSTEC, Yokohama, Japan
[11]Royal Netherlands Meteorological Institute (KNMI), Atmospheric Composition Research, De Bilt, the Netherlands
*now at: University of Cambridge, Centre for Atmospheric Science, Cambridge, UK

Received: 1 August 2006 – Accepted: 16 August 2006 – Published: 12 September 2006

Correspondence to: V. Eyring (Veronika.Eyring@dlr.de)

Abstract

The global impact of shipping on atmospheric chemistry and radiative forcing, as well as the associated uncertainties, have been quantified using an ensemble of ten state-of-the-art atmospheric chemistry models and a pre-defined set of emission data. The analysis is performed for present-day conditions (year 2000) and for two future ship emission scenarios. In one scenario emissions stabilize at 2000 levels; in the other emissions increase with a constant annual growth rate of 2.2% up to 2030 (termed the "Constant Growth Scenario"). The first key question addressed by this study is how NO_x and SO_2 emissions from international shipping might influence atmospheric chemistry in the next three decades if these emissions increase unabated. The models show future increases in NO_x and ozone burden which scale almost linearly with increases in NO_x emission totals. For the same ship emission totals but higher emissions from other sources a slightly smaller response is found. The most pronounced changes in annual mean tropospheric NO_2 and sulphate columns are simulated over the Baltic and North Seas; other significant changes occur over the North Atlantic, the Gulf of Mexico and along the main shipping lane from Europe to Asia, across the Red and Arabian Seas. Maximum contributions from shipping to annual mean near-surface ozone are found over the Atlantic (5–6 ppbv in 2000 reaching up to 8 ppbv in the 2030 Constant Growth Scenario). Large increases in tropospheric ozone column are found over the Atlantic and even stronger over the Indian Ocean (1 DU in 2000 and up to 1.8 DU in 2030). Tropospheric ozone forcings due to shipping are 9.8±2.0 mW/m^2 in 2000 and 13.6±2.3 mW/m^2 in 2030. Whilst increasing ozone, ship NO_x simultaneously enhances OH, reducing the CH_4 lifetime by 0.13 yr in 2000, and by up to 0.17 yr in 2030, introducing a negative radiative forcing. Over Europe, the increase in ship emissions under the "Constant Growth Scenario" will enhance the positive trend in NO_2 over land up to 2030. In addition, efforts to lower European sulphate levels through reductions in SO_2 emissions from anthropogenic sources on land will be partly counteracted by the rise in ship emissions. Globally, shipping contributes with 3% to increases in ozone

ACPD

6, 8553–8604, 2006

burden until 2030 and with 4.5% to increases in sulphate. The results discussed above are calculated under the assumption that all other emissions follow the IPCC SRES A2 scenario. However, if future ground based emissions follow a more stringent scenario, the relative importance of ship emissions becomes larger. The second key issue of this work is to examine the range of results given by the individual models compared to the ensemble mean. Uncertainties in the different model approaches in the simulated ozone contributions from ships are found to be significantly smaller than estimated uncertainties stemming from the ship emission inventory, mainly the ship emission totals, the neglect of ship plume dispersion, and the distribution of the emissions over the globe.

1 Introduction

Seagoing ships emit exhaust gases and particles into the marine boundary layer contributing significantly to the total budget of anthropogenic emissions from the transportation sector (e.g. Olivier et al., 2001; Eyring et al., 2005a). Emissions of nitrogen oxides and other ozone precursors from shipping lead to tropospheric ozone formation and perturb the hydroxyl radical (OH) field, and hence the lifetime of methane (CH_4), which changes the Earth's radiation budget as ozone and methane are greenhouse gases. Evidence for the importance of ship emissions comes from satellite observations from GOME (Beirle et al., 2004) and SCIAMACHY (Richter et al., 2004) that show enhanced tropospheric NO_2 columns along the major international shipping routes in the Red Sea and over the Indian Ocean. A number of atmospheric model studies quantifying the impact of ship emissions on the chemical composition of the atmosphere and on climate have been published in recent years. All these studies used a global fuel consumption of about 150 million metric tons (Mt, or Tg) per year derived from energy statistics (Corbett and Fischbeck, 1997; Corbett et al., 1999; Olivier et al., 2001; Endresen et al., 2003). However, recent estimates of the fuel consumption calculated with an activity-based approach suggest higher fuel consumption of around

ACPD
6, 8553–8604, 2006

280 Mt (Corbett and Köhler, 2003; Eyring et al., 2005a). Even though existing model studies used the lower total fuel consumption, it has been shown that models overestimate the observed NO_x distribution for example over the Atlantic (Lawrence and Crutzen, 1999; Kasibhatla et al., 2000; Davis et al., 2001; Endresen et al., 2003), but underestimate SO_2 observations (Davis et al., 2001).

It is now believed that the discrepancy between measured and modelled NO_x can be reduced by accounting for ship plume dispersion in global models (Kasibhatla et al., 2000; Davis et al., 2001; Song et al., 2003; von Glasow et al., 2003; Chen et al., 2005). In ship plumes the lifetime of NO_x is significantly reduced compared to the background and NO_x in the plume is rapidly converted before it can be diluted to the grid size of global models (Kasibhatla et al., 2000; Chen et al., 2005). In order to consider chemical and microphysical processes of sub-scale effects in a global atmospheric model with a horizontal resolution typically of the scale between 100 and 500 km, the processes have to be parameterised, e.g. by the use of effective emission indices depending on the meteorology and background conditions. However, there is no clear consensus on the effective global emissions from ships. In this study we use relatively low global emission estimates, to implicitly account for plume effects.

In addition to NO_x, shipping contributes significantly to global SO_2 emissions as the average sulphur content of the fuel burned in marine diesel engines of 2.4% is high compared to other transport sectors (EPA, 2002). In large areas of the Northern Hemisphere SO_2 emissions from ships are comparable to biogenic dimethyl sulphide (DMS) emissions, which are the main natural source of sulphur over the oceans (Corbett et al., 1999; Capaldo et al., 1999; Derwent et al., 2005). The main oxidation processes for SO_2 are believed to be either via OH in the gas phase or in the liquid phase via O_3 or H_2O_2 in cloud droplets (Langner and Rohde, 1991). As SO_2 is primarily controlled by aqueous processes, it is expected that SO_2 is largely independent of plume chemistry (Davis et al., 2001). The increase in sulphate concentration has a direct and indirect effect on climate. The direct effect results from enhanced scattering of solar radiation (Haywood and Shine, 1995). The indirect effect of sulphate particles (SO_4)

from shipping results from changes in the microphysical, optical and radiative properties of low marine clouds. These modified clouds can be identified as long curves in satellite images, known as ship tracks (e.g. Scorer, 1987; Durkee et al., 2000).

The world merchant fleet in terms of numbers of ships has been substantially increased by 35% over the past 50 years, accompanied by a significant increase in emission totals (Eyring et al., 2005a). At the end of the year 2001 it consisted of around 90 000 ocean-going ships of 100 gross tons (GT) and above (Lloyd's, 2002). Shipping is currently one of the less regulated sources of anthropogenic emissions with a high reduction potential through technological improvements, alternative fuels and ship modifications. Emission scenario calculations up to the year 2050 show that if no control measures are taken beyond existing International Maritime Organization (IMO) regulations (International Maritime Organization, 1998), NO_x emissions might increase with an annual growth rate of 1.7% between 2000 and 2030 and up to a value of present day global road transport by 2050 (38.8 Tg (NO_2)/yr) (Eyring et al., 2005b). If the sulphur content remains at present day levels a doubling of ship SO_2 emissions can be expected. However, given the air quality issue of shipping emissions, further emission reductions of total NO_x and SO_2 emissions are likely. Using aggressive NO_x emission reduction technologies, a significant decrease up to 85% of today's NO_x emissions could be reached through technological improvements by 2050, in spite of a growing fleet. A detailed summary of current national and international maritime regulations is given in Eyring et al. (2005b).

Currently there is a large uncertainty about the overall impact of emissions from international shipping which needs to be explored using global atmospheric modelling. The first key question addressed in this study is how the emissions of international shipping might influence atmospheric chemistry, in particular tropospheric ozone and sulphate, in the next three decades, if these emissions increase unabated. To address this, impacts of NO_x and SO_2 emissions from international shipping are assessed with the help of an ensemble of state-of-the-art global atmospheric chemistry models. The second major issue is to examine the range of results given by the individual models

ACPD
6, 8553–8604, 2006

EGU

compared to the ensemble mean to give an estimate of the uncertainties introduced by different modelling approaches. The participating models have also been evaluated and used in accompanying studies (e.g. Stevenson et al., 2006; Dentener et al., 2006a, b; Shindell et al., 2006, van Noije et al., 2006) as part of the European Union project ACCENT ("Atmospheric Composition Change: the European NeTwork of excellence"; http://www.accent-network.org).

The models and model simulations used in this study together with the method to analyse the results are described in Sect. 2. Large-scale chemistry effects on NO_2 and ozone distributions due to NO_x emissions from ships are discussed in Sect. 3.1 for present-day conditions and in Sect. 3.2 for 2030, while impacts of SO_2 emissions from ships on sulphate distributions are discussed in Sect. 3.3. In Sect. 3.4 radiative forcings (RFs) from tropospheric ozone calculated with the help of an offline radiation code are summarised and RFs due to CO_2 and sulphate are estimated. Section 4 discusses possible uncertainties in the presented results mainly stemming from the emission inventory itself, the neglect of plume chemistry and assumptions in the future scenarios for background as well as ship emissions. Section 5 closes with a summary and conclusions.

2 Models and model simulations

2.1 Participating models

Ten global atmospheric chemistry models have participated in this model intercomparison. Seven of the ten models are Chemistry-Transport Models (CTMs) driven by meteorological assimilation fields and three models are atmospheric General Circulation Models (GCMs). Two of the GCMs are driven with the dynamical fields calculated by the GCM in climatological mode, but the fully coupled mode (interaction between changes in radiatively active gases and radiation) has been switched off in the simulations of this study. The other GCM runs in nudged mode, where winds and tem-

ACPD
6, 8553–8604, 2006

perature fields are assimilated towards meteorological analyses. Therefore, changes in the chemical fields do not influence the radiation and hence the meteorology in any of the model simulations used here; so for a given model, each scenario is driven by identical meteorology. The main characteristics of the ten models are summarised in Table 1 and the models are described in detail in the cited literature.

The horizontal resolution ranges from 5.6°×5.6° (MATCH-MPIC) to 2.8°×2.8° (CHASER-CTM, FRSGC/UCI, UIO_CTM2) and 3°×2° (TM4). The vertical resolution varies in terms of number of vertical layers and upper boundary and ranges from 9 layers with a model top at 100 hPa (STOCHEM-HadAM3) to 52 layers with a model top at 0.006 hPa (GMI/CCM3).

All models use detailed tropospheric chemistry schemes even though notable differences exist between the models, e.g. in the hydrocarbon chemistry. Of the ten models, four included the tropospheric sulphur cycle (CHASER-CTM, STOCHEM-HadAM3, STOCHEM-HadGEM, and TM4). These models include anthropogenic and natural sulphur sources, and account for oxidation in the gas phase by OH, and in the aqueous phase (in cloud droplets) by H_2O_2 and O_3. Sulphate aerosol is predominantly removed by wet-deposition processes. Models also differ in the representation of cloud processes and hydrological processes and a variety of different advection schemes are used.

Differences in the main characteristics as listed above will lead to differences in the modelled response to NO_x and SO_2 emissions from shipping, even if near-identical forcings (e.g., sea surface temperatures, natural and anthropogenic emissions, and meteorology) are used. A more detailed discussion of the sources of differences between the models is included in Stevenson et al. (2006).

The models have been evaluated in accompanying studies. For example, ozone fields have been compared to ozone-sonde measurements (Stevenson et al., 2006), NO_2 columns have been compared to three state-of-the-art retrievals from measurements of the Global Ozone Monitoring Experiment (van Noije et al., 2006), CO has been compared to near-global observations from the MOPITT instrument and local sur-

face measurements (Shindell et al., 2006), deposition budgets have been compared to nearly all information on wet and dry deposition available worldwide (Dentener et al., 2006b), and finally modelled surface ozone fields have been compared to observations from various measurement sites (Dentener et al., 2006a). In all these studies, the ensemble mean was among the best when comparing to measurements. In this study we build on the model evaluation work listed above as well as on the individual evaluation of the models and make the assumption that the models produce reasonable simulations of the key chemical species. We use the ensemble mean to assess large-scale chemistry effects resulting from ship emissions for the present day and in the future.

2.2 Model simulations

Two of the five simulations that have been defined as part of the wider PHOTOCOMP-ACCENT-IPCC study have been used in this work: a year 2000 base case (S1) and a year 2030 emissions case (S4) following the IPCC (Intergovernmental Panel on Climate Change) SRES (Special Report on Emission Scenarios) A2 scenario (Nakicenovic et al., 2000). Full details on the emissions used in the S1 and S4 simulations are summarised in Stevenson et al. (2006) and only the key aspects for this study are given here.

To retain consistency with all other emissions, ship emissions in the year 2000 (S1) are based on the EDGAR3.2 dataset (Olivier et al., 2001) at a spatial resolution of 1° latitude×1° longitude. The global distribution of ship emissions in EDGAR3.2 is based on the world's main shipping routes and traffic intensities (Times Books, 1992; IMO, 1992). EDGAR3.2 includes data for 1995, which have been scaled to 2000 values assuming a growth rate of 1.5%/yr, resulting in annual NO_x and SO_2 emissions of 3.10 Tg(N) and 3.88 Tg(S), respectively, similar to the emission totals published by Corbett et al. (1999). Table 2 summarises the global annual anthropogenic surface emission and ship emission totals for NO_x and SO_2. In the 2000 simulation (S1), ship emissions account for about 11.2% of all anthropogenic surface nitrogen oxide emissions and for about 7.2% of all anthropogenic sulphur emissions. Other emissions from

ships such as CO, particulate matter, methane (CH_4) and non-methane hydrocarbons (NMHCs) were not included in this inventory and were therefore not considered in this study. However, Endresen et al. (2003) showed that the effects of CH_4 and NMHC emissions from ships on ozone are very small. The effect of CO emitted by ships is also expected to be small, as large marine vessels emit very little CO (Eyring et al., 2005a).

As noted in Stevenson et al. (2006) in the S4 simulation emissions from ships were included at year 2000 levels by mistake. All other anthropogenic sources (except biomass burning emissions, which remain fixed at year 2000 levels) vary according to A2 broadly representing a "pessimistic" future situation. The simulation S4 is used in this study to assess the impact of ship emissions under different background levels. An additional model simulation for 2030 (S4s) has been designed to assess the impact of shipping if emission growth remains unabated. Ship emissions in S4s are based on a "Constant Growth Scenario" in which emission factors are unchanged and emissions increase with an annual growth rate of 2.2% between 2000 and 2030. In the S4s scenario emissions from shipping increase to 5.95 Tg(N) for NO_x and 7.36 Tg(S) for SO_2 in 2030. Note that the only difference between the scenarios S4 and S4s is that S4 uses 2000 ship emissions whereas S4s includes an increase in ship emissions. As an example, the global distribution of surface NO_x emissions for the years 2000 (S1) and 2030 (S4s) is displayed in Fig. 1. Vessel traffic distributions are assumed to stay the same for all model simulations presented here.

To assess the impact of ship emissions on chemistry and climate in 2000 and 2030, two sensitivity simulations have been defined that use identical conditions to S1 or S4/S4s except that ship emissions are excluded. The year 2000 and 2030 experiments without ship emissions are denoted as S1w and S4w.

All 2030 model experiments (S4, S4s and S4w) are driven by the same meteorological data as the 2000 simulations (S1 and S1w). Global methane mixing ratios have been specified across the model domain (1760 ppbv in 2000 and 2163 ppbv in 2030) to save time spinning up the models and to help constrain the results (for details see

ACPD
6, 8553–8604, 2006

EGU

Stevenson et al., 2006). Nine of the ten models performed single year simulations with spin-ups of at least 3 months and one model (STOCHEM-HadGEM) performed a four year simulation. For the multi-annual simulations the results have been averaged over all four years to reduce the effects of inter-annual variability.

2.3 Model analyses

Each model provided output for 3-D monthly mean NO_x, ozone and sulphate mixing ratios as well as the mass of each grid-box on the native model grid for all five simulations. As models used a variety of vertical co-ordinate systems and resolutions, the output has been converted to a common vertical grid. To be comparable to the results reported in Stevenson et al. (2006) we use the same grid and method to mask the tropopause. Model results are interpolated to the 19 hybrid (sigma-pressure) levels of the Met Office HadAM3 model where up to 14 of these levels span the troposphere. Results were also interpolated to a common horizontal resolution of $5^\circ \times 5^\circ$. However, for the comparison of model results to tropospheric NO_2 columns measured by SCIAMACHY, the models have been interpolated to a finer horizontal resolution of $0.5^\circ \times 0.5^\circ$. To calculate the ensemble mean on the common grid the simulated fields have been masked at the chemical tropopause (O_3=150 ppbv) similar to the method applied in Stevenson et al. (2006). For the 2000 simulations (S1 and S1w) we apply a consistent mask by using the ozone field from the S1w simulation for each model and all species. For the 2030 simulations (S4, S4s, and S4w) the S4w ozone field is used to mask the tropopause. To calculate global tropospheric burdens, model results were masked in the same way (O_3=150 ppbv) but summed on their native grids, to avoid the introduction of errors associated with the interpolation (Sect. 3.2). The impact of ship emissions on NO_x, ozone and sulphate distributions is assessed by calculating the difference between the reference simulation (S1 for 2000; S4 or S4s for 2030) and the ensemble mean of the no-ships scenario (S1w for 2000; S4w for 2030). For the calculation of instantaneous tropospheric ozone forcings the differences in ozone fields

between sensitivity and reference simulations on the common grid were used.

3 Results

3.1 Large-scale chemistry effects of NO_x ship emissions in 2000

To examine the range of results given by the individual models compared to the ensemble mean, Fig. 2 shows differences in annually averaged zonal mean ozone versus height between the 2000 base case simulation (S1) and the model simulation without shipping (S1w) for each model and the ensemble mean. Standard deviations are shown in addition indicating regions of large intermodel variability. All models show the maximum contributions from ships in zonal annual mean near-surface ozone in northern mid-latitudes between 10° N and 55° N, where most of the global ship emissions are released into the atmosphere (see Fig. 1). A rapid decrease of the impact on ozone distributions with height is simulated. There are notable differences in the magnitude of the response to ship emissions between the individual models which can be attributed to differences in the main characteristics of the models (see Sect. 2.1) or to slightly different background emissions (see Stevenson et al., 2006). The two models that show the strongest response of ozone to ship emissions are the UIO_CTM2 and the STOCHEM-HadAM3 models; the ones with the weakest response are the LMDz/INCA-CTM and the TM4 models. Previous studies reported that the production of ozone depends on the resolution of the model with models having higher resolution simulating less ozone production than those with a coarser resolution (e.g. Esler, 2003; Wild and Prather, 2006). However, there are large differences in the responses of the UIO_CTM2, CHASER and FRSGC/UCI models, all running at the highest resolution used here (2.8°×2.8°), while the MATCH-MPIC model running at the coarsest horizontal resolution (5.6°×5.6°) has a low ozone response. It is therefore clear that factors other than resolution play an important role in explaining the differences. For example, the parameterisation of sub-grid scale convection has been shown to be important and

ACPD
6, 8553–8604, 2006

differences in the cloud processing, dry and wet deposition, boundary layer mixing or the chemical reactions considered likely also play a role. The ensemble mean shows the largest increase in near-surface zonal mean ozone due to ships of up to 1.3 ppbv in northern mid-latitudes with intermodel differences around 20% (Figs. 2k, l). In the free troposphere at latitudes further north changes still reach 1 ppbv with intermodel differences of around 0.16 ppbv (16%). In the Southern Hemisphere no significant changes in zonal mean ozone distribution are simulated in all models. We conclude that the range of results given by the individual models indicates uncertainties of the presented ensemble means of the order of 20% near the surface and slightly lower in the free troposphere. The high standard deviations in the tropical tropopause layer are due to a single model (CHASER). The main conclusions in the subsequent sections are based on the models' ensemble mean.

Despite the fact that there are no seasonal variations in the ship emission inventory, the simulated ozone response shows some seasonal variability. Figure 3 displays absolute and relative changes in the ensemble mean near-surface NO_2 and ozone distributions between the S1 and the S1w simulation in January (left) and July (right). Due to the short lifetime of NO_2 in the boundary layer, near-surface changes in NO_2 follow closely the main shipping routes, but the dispersion is a few hundred kilometres, which is partly due to coarse resolutions of the models, but also transport. Maximum changes of 2.3 ppbv are found over the Baltic Sea in both months. In the English Channel and along the west coast of Europe (from Ireland to Morocco) NO_2 changes are also significant (around 0.5 ppbv). Enhanced NO_2 levels up to 0.2 ppbv are also simulated over large areas of the Atlantic and e.g. in the Red Sea and along the main shipping lane to the southern tip of India, to Indonesia and north towards China and Japan as well as in the Gulf of Mexico. In July NO_2 changes are in general slightly smaller than in January and cover a smaller area. For example, over the Atlantic and Europe, as the lifetime of NO_x in the summer months is shorter due to higher chemical activity. Relative changes in NO_2 strongly depend on the background conditions. For example, even though absolute NO_2 changes over the Baltic and the North Sea are large, relative changes are

ACPD
6, 8553–8604, 2006

EGU

less pronounced because of high background NO_2 levels. The largest relative changes of up to 80% in January and 96% in July are found over the remote Atlantic and along the major shipping lanes, where background levels are small and NO_x emissions from ships are the dominant source (see Fig. 1).

Substantial differences are simulated between the near-surface January and July ensemble mean ozone changes (Fig. 3, lower panels). The reason for the difference is that in winter time additional NO_x emissions from shipping lead to ozone titration in the highly polluted regions over the continents, whereas in summer the additional NO_x leads to ozone production. Ozone concentrations in January show a decrease of around 1 ppbv with maximum decreases of up to 2.8 ppbv over the Baltic. The changes in July over this region are rather small but positive. The largest increases in January are found southward of 30° N, where the available solar radiation is sufficient for ozone production to outweigh direct removal of NO. Most pronounced increases of 3.3 ppbv are simulated over the Indian Ocean and along the main shipping lane west of the coast of Southern Africa. The simulated large decrease in ozone over a large area in Europe in winter, which has not been reported in e.g. the Endresen et al. (2003) study, might be due high vessel traffic densities in particular over the Baltic Sea in the inventory used here. Vessel traffic densities derived from different sources such as AMVER (Automated Mutual-assistance Vessel Rescue system) or the Purple Finder (PF) data set (available at http://www.purplefinder.com) report fewer observations there (Endresen et al., 2003).

In July, the geographical pattern in ozone changes is similar to the pattern in Lawrence and Crutzen (1999) showing most pronounced changes over wide areas of the Atlantic up to 12 ppbv (approx. 35%) and over the Western and Northern Pacific up to 5 ppbv (approx. 25%). Changes of the order of 5 ppbv (approx. 10%) are also simulated over the Indian Ocean. The simulated changes over the Atlantic and the Indian Ocean are in good agreement with results reported in Endresen et al. (2003), but smaller over the Pacific. Differences between the two studies are likely related to the difference in vessel traffic densities (see Sect. 4.1). Due to the longer lifetime of

ACPD
6, 8553–8604, 2006

EGU

ozone compared to NO_2 in the boundary layer, ozone changes are less tightly tied to the main shipping lanes compared to NO_2 changes, and affect larger areas. Non-linear effects of ozone photochemistry are significant. For example, over the Baltic and the North Sea, where background NO_2 levels are relatively high, changes in ozone are comparatively small, whereas they are substantial over more remote areas.

The peak response in the ensemble mean NO_2 column due to shipping revealed from the difference between the S1 and S1w ensemble mean is simulated over the Baltic Sea, reaching up to 2.5×10^{15} molecules/cm^2 in 2000 (not shown). Large changes are also simulated over a wide area of the Atlantic (up to 0.7×10^{15} molecules/cm^2) as well as over the main shipping lane from Europe to Asia and in the Gulf of Mexico. Peak values of about 0.4×10^{15} molecules/cm^2 are found in these regions. Recently, enhanced tropospheric NO_2 columns have been observed over the Red Sea and along the main shipping lane to the southern tip of India, to Indonesia and north towards China and Japan (Beirle et al., 2004; Richter et al., 2004). Here we intercompare the tropospheric NO_2 columns derived from SCIAMACHY nadir measurements from August 2002 to April 2004 (Richter et al., 2004) to the ensemble mean in 2000 (S1 simulation). The ensemble mean in Fig. 4 consists of the eight models that provided tropospheric NO_2 columns at 10:30 a.m. local time, which is close to the overpass time of the ERS-2 satellite. The two STOCHEM models provided output only as 24 h mean, and are not included in the ensemble mean shown in Fig. 4. To compare the model data to the satellite measurements, individual model results and SCIAMACHY data were interpolated to a common grid ($0.5^\circ\times0.5^\circ$). The models simulate similar tropospheric NO_2 columns over the remote ocean as observed by SCIAMACHY and also reproduce the overall pattern of the geographical distribution reasonably well. However, although the shipping signal is clearly visible in the satellite data it is not resolved by the models, because the intercomparison of modelled and observed NO_2 columns is complicated by several factors. First of all, the spatial resolution of the SCIAMACHY measurements (30×60 km^2) is much higher than that of the global models (typically $5^\circ\times5^\circ$) leading to higher NO_2 values in the localized plumes from ship emissions. Secondly, in the

ACPD
6, 8553–8604, 2006

EGU

particular scene shown in Fig. 4, shipping routes are rather close to land. Given the low resolution of the models, the grid boxes close to the coast are dominated by NO_x emissions from land sources which are much stronger than emissions from shipping. Thus, the shipping signal cannot be identified in the coarse resolution model data. From this point of view, an intercomparison over the remote ocean (e.g. over the Atlantic) far away from any land source would be preferable. However, up to now, no statistically significant satellite data on ship emissions are available for remote oceans.

3.2 Large-scale chemistry effects of NO_x ship emissions in 2030

3.2.1 Ozone distributions

Figure 5 shows modelled ensemble mean ozone changes due to ship emissions for the year 2000 (S1–S1w) and for two different scenarios in 2030 (S4–S4w; S4s–S4w). As vessel traffic densities are the same in all model simulations the 2030 results mainly show a scaling of the 2000 results, but non-linearity effects also play a role.

Ozone changes versus height in 2000 (Fig. 5a) have already been discussed in Sect. 3.1. The largest ozone response is found near the surface between 10–55° N, and rapidly decreases with altitude. Keeping emissions from shipping at 2000 levels but with all other emissions increasing, the pattern in zonal mean changes remains the same but the impact is slightly less than in 2000 due to lower O_3 production rates under the influence of higher background of NO_x (Fig. 5d; S4–S4w). Under the S4s scenario near-surface ozone changes of about 1.7 ppbv are simulated in the zonal mean between 10–55° N, and even in the free troposphere changes in ozone reach up to 1.3 ppbv (Fig. 5g).

Changes in the annual mean near-surface level reach 5.5 ppbv over the Atlantic (Fig. 5b) and increase up to 7.4 ppbv in the S4s scenario in 2030 (Fig. 5h). Over Northern Europe where there are high levels of NO_x, and relatively low levels of insolation (even in summer), the increase in NO_x from shipping decreases, rather than increases, ozone levels. This is due to reduction in oxidant levels as OH is removed by

the reaction NO_2 + OH → HNO_3, and in winter to direct titration of ozone by NO_2. The effect is stronger in the 2030 scenarios due to the increased background level of NO_x in Northern Europe, with shipping decreasing ozone by 3 ppbv in the S4s scenario.

The most pronounced changes in tropospheric ozone columns are found over the Indian Ocean (1.16 DU in 2000 and 1.72 DU in 2030), related to the higher tropopause there and to more effective transport of ozone from the boundary into the upper troposphere. A second peak is simulated over the Atlantic (Figs. 5c, f, i).

3.2.2 Linearities in NO_x and O_3 burden response to ship emissions

Changes in annual mean NO_x and ozone burdens are calculated for the two 2030 scenarios (S4–S4w; S4s–S4w) as described in Sect. 2.3 for four different regions (global mean, Atlantic Ocean, Baltic Sea, and Indian Ocean; see Fig. 6). A linear regression is performed for the changes in NO_x and O_3 burdens due to shipping over the three scenarios S4w, S4 and S4s and the origin (zero NO_x ship emissions/zero changes in NO_x and O_3 burdens). The changes in global tropospheric NO_x burden associated with these two scenarios show a fairly linear relationship for all models (Fig. 7, left), and a doubling of NO_x emissions approximately results into a doubling of the ensemble mean NO_x burden.

For ozone the correlation is also broadly linear (Fig. 7, right). Only small saturation effects are visible as the ozone burden for the low emission scenario (3.10 Tg(N)) lies above the multi-regression line whereas the one for the high emission scenario (5.95 Tg(N)) lies below the multi-regression line for all models. This is to be expected due to non-linearities in the ozone chemistry. In contrast to the relatively small degree of saturation computed here, Labrador et al. (2004) computed a substantial saturation effect for lightning NO_x emissions as they were increased from 0 to 20 Tg(N)/yr, with the saturation already becoming clearly evident between 5 and 10 Tg(N)/yr. Although there are only three data points available here (0, 3.1 and 5.95 Tg(N)/yr), there is evidence in these results that the ship NO_x effect is only weakly subject to saturation in its current magnitude range, and that saturation cannot be expected to help mitigate

ACPD
6, 8553–8604, 2006

the effects of near-future increases. Overall, similar to NO_x burdens, a doubling in NO_x ship emissions results in approximately a doubling in ozone burdens in the ensemble mean. Note that, whereas the majority of the models (eight out of ten) show similar response, the two STOCHEM models simulate NO_x burden changes around a factor of 3 (STOCHEM-HadAM3) or 6 (STOCHEM-HadGEM) higher than the other models, which explains the large standard deviations of the ensemble mean NO_x burden. As further discussed below, this can mainly be attributed to the wintertime chemistry in these two models. For the annual ozone burdens the two STOCHEM models show similar results compared to all other models, why the inter-model standard deviations for ozone are small (<15%).

Similar to the global annual burdens, eight out of the ten models show similar response in the seasonal cycle of NO_x and ozone burden changes for the S4s–S4w scenario over the Atlantic Ocean, the Baltic Sea, the Indian Ocean and globally (Fig. 8). As expected, the seasonal cycle in both NO_x and ozone is most pronounced in the Baltic Sea (northern hemispheric mid-latitudes), whereas the seasonal cycle in the Indian Ocean is relatively small. Two of the ten models (STOCHEM-HadGEM and STOCHEM-HadAM3, both using the same chemistry scheme) show significantly higher changes in NO_x burdens in winter time in northern mid-latitude regions (Atlantic and Baltic Sea). An additional analysis showed that the reason for the high changes in NO_x burdens in winter in the two STOCHEM models is likely related to an accumulation of NO_x in the Arctic in winter. An improved representation of the heterogeneous NO_x loss shows dramatic decreases in northern winter NO_x, which improves the consistency with the other models shown here (M. Sanderson, personal communication), but this scheme has not been applied to the model simulations used in this study. The change in ensemble mean ozone burdens reach peak values of 0.9 Tg over the Atlantic in August, 0.25 Tg over the Indian Ocean in October, and 0.04 Tg over the Baltic Sea in June.

The global change in NO_x burden due to ship emissions as simulated by the ensemble mean in the S4s scenario is enhanced by 25 Gg in summer. The global ozone burden is enhanced by about 4 Tg with peak changes in October and smallest changes

in January.

3.3 Large-scale chemistry effects of SO_2 ship emissions in 2000 and 2030

Large amounts of SO_2 are emitted by international shipping which is expected to enhance sulphate levels (e.g. Capaldo et al., 1999; Endresen et al., 2003). SO_2 can be removed from the atmosphere by wet and dry deposition or oxidised to sulphate. Two important oxidation mechanisms exist, namely the reaction of SO_2 with OH forming sulphuric acid (H_2SO_4) in the gas phase, and the oxidation of SO_2 e.g. by O_3 or hydrogen peroxide (H_2O_2) in the liquid phase of cloud droplets forming H_2SO_4 and ammonium sulphate. H_2SO_4 in the gas phase can condense on pre-existing aerosol particles such as sea salt resulting in an increase of particle mass or form new aerosols by nucleation. SO_4 produced within cloud droplets is released into aerosol phase once the cloud evaporates. Thus, SO_2 emitted by shipping changes the chemical composition of the aerosol by increasing sulphate concentrations. In addition, aerosol size distribution and particle number concentration of the background aerosol are modified. These changes in the physical and chemical properties of the aerosol result in modified absorption and scattering of solar radiation (direct aerosol effect) and changes in cloud microphysical properties through changes in properties of the cloud condensation nuclei (indirect aerosol effects). Thus, although SO_2 is not radiatively active, SO_2 emissions impact on climate by formation of SO_4 modifying basic aerosol properties.

A subset of four models (CHASER, STOCHEM-HadAM3, STOCHEM-HadGEM, and TM4) included a detailed sulphur cycle. The ensemble mean of these four models has been applied to quantify changes due to shipping in sulphate distributions now and in the future. Figure 9 shows the modelled ensemble mean SO_4 change for the years 2000 (scenario S1–S1w) and 2030 (scenarios S4–S4w, S4s–S4w). Maximum changes are located in the boundary layer of the northern mid-latitudes around 40° N. These changes result in about 30 pptv in the year 2000 simulations and 50 pptv in the year 2030 (S4s–S4w). With increasing height, the changes in SO_4 decrease continuously to about 3–5 pptv (2000) and 6–9 pptv (2030) in the upper troposphere. In the

lowermost boundary layer over the Atlantic Ocean at the west coast of Europe and over the Baltic Sea, maximum annual sulphate changes amount to about 200 pptv in 2000 and 300 pptv in 2030. The geographical pattern shows the main shipping routes over the Atlantic Ocean between Europe and North America and over the Red Sea and the Indian Ocean between the Arabian Peninsula and India. In all other parts of the world, changes in sulphate due to SO_2 emissions from shipping remain low in general. Globally, shipping contributes with 4.5% to sulphate increases until 2030 under the "Constant Growth Scenario".

3.4 Radiative forcing

Ozone distributions from all scenarios and all models were inserted into an offline radiation code (Edwards and Slingo, 1996), with all other parameters held constant, broadly representing the present-day atmosphere. In the stratosphere, ozone was overwritten by a climatology, so the changes discussed here are purely tropospheric. Comparing instantaneous short-wave and long-wave radiative fluxes at the tropopause between scenarios yields ozone radiative forcings (see Stevenson et al., 1998 for more details on the method). The code includes effects of clouds, but does not include stratospheric temperature adjustment. Previous studies with this set up have consistently found a 22% reduction in the instantaneous forcing compared to the equivalent forcing with stratospheric adjustment. Following Stevenson et al. (2004) we apply the 22% as a constant correction, to make the ozone forcings directly comparable to methane and CO_2 forcings from the same scenarios. Figure 10a shows maps of multi-model ensemble mean annual mean instantaneous ozone radiative forcings for the 2030 high emissions case (S4s) relative to the scenario without ships (S4w). Similar distributions were found for the other scenarios. The peak forcing occurs over the Indian Ocean, the site of the largest column ozone changes (Fig. 5), but also a region with relatively high surface temperatures, and a high, cold tropopause. A secondary peak occurs over the Caribbean for similar reasons. Further north over the Atlantic the forcing is less, despite a significant ozone change, reflecting the smaller surface-to-tropopause

ACPD
6, 8553–8604, 2006

EGU

temperature contrast and increasing cloudiness.

Figure 10b shows the inter-model standard deviation, which is typically 15–25%. The ensemble mean forcings and standard deviations for the three cases (S1–S1w, S4–S4w and S4s–S4w), applying a 22% reduction to account for stratospheric temperature adjustment, are 9.8±2.0, 7.9±1.4 and 13.6±2.3 mW/m^2, respectively. The influence of ship emissions on the ozone forcing slightly reduces as the background ozone levels rise, but the relationship between ship NO_x emissions and resultant O_3 forcing is close to linear. Comparing with the total ozone forcing between 2000 and 2030, as discussed in Stevenson et al. (2006), the contribution from ships in the S4s case to the global projected tropospheric ozone forcing is 4%.

Ship NO_x emissions also affect the radiatively active gas methane, by increasing OH and reducing the methane lifetime. Five models (CHASER-CTM, FRSGC/UCI, LMDzINCA, STOCHEM-HadAM3 and TM4) provided methane destruction fluxes for each scenario, and these were used to calculate whole atmosphere CH_4 lifetimes, as described in Stevenson et al. (2006). For four of the five models, changes in lifetime between scenarios were very consistent (within 4% of each other), but STOCHEM-HadAM3 was nearly twice as sensitive, and considered an outlier. Here we use ensemble mean results from the four models to assess ship impacts on CH_4 lifetime. For present-day, ship NO_x shortens the CH_4 lifetime by 0.13 yr (1.56±0.05%) (S1-S1w); in 2030 the same ship NO_x perturbation reduces the lifetime by 0.10 yr (1.14 ± 0.02%) (S4-S4w), again illustrating the slightly lower sensitivity when background levels are higher. Following the "Constant Growth Scenario" the methane lifetime is reduced by an additional 0.07 yr (0.77±0.02%) in 2030 (S4s-S4). Ship NO_x therefore introduces a negative radiative forcing by reducing the build-up of methane. A full calculation of the magnitude of the negative forcing from this mechanism is not included here, but globally it is expected to probably outweigh the positive ozone forcing (e.g., Wild et al., 2001).

The various contributions to the radiative forcing from shipping also include radiative forcing due to CO_2 and sulphate changes. The corresponding radiative forcing

of CO_2 is estimated from the fraction of the ship emission totals in the year 2000 (136.7 Tg(C)/yr, Endresen et al. (2003)) to the total annual CO_2 emissions in 2000 (7970 Tg(C)/yr; IPCC, 2001; scenario A2). This fraction (1.7%) is used to scale the RF resulting from all CO_2 sources (1.51 W/m^2; IPCC, 2001; scenario A2, ISAM reference case) linearly, resulting in a RF of 26 mW/m^2 due to shipping. The same approach is used to estimate CO_2 RF for the year 2030, with annual emissions of 14 720 Tg(C)/yr for all sources (IPCC, 2001; scenario A2) and a total CO_2 RF of 2.59 W/m^2 (IPCC, 2001; scenario A2, ISAM reference case). The emissions from shipping are assumed to increase at an annual rate of 2.2% since 2000, resulting in 262.6 Tg(C)/yr in 2030. For the simulation S4, shipping contributes with 0.9% to the total annual CO_2 emissions, for S4s with 1.8%. This results in CO_2 RF of about 24 mW/m^2 (S4–S4w) and 46 mW/m^2 (S4s–S4w) due to shipping in 2030. However, since CO_2 has a long average lifetime, the time integral of ship emissions would be needed to estimate a more accurate number for RF. Thus calculations with a linear response model similar to the RF estimates for aviation (Sausen and Schumann, 2000) will give more accurate results.

Direct sulphate forcings are calculated from the change in total SO_4 burdens due to shipping. The relative change of the SO_4 burdens is used to scale the total direct radiative forcing of sulphate particles given by IPCC (2001) (scenario A2) of –0.4 W/m^2 for the year 2000 and –0.65 W/m^2 for the year 2030. The relative contribution of shipping to the total sulphate burdens is about 3.6% (S1–S1w), 2.0% (S4–S4w), and 4.0% (S4s–S4w). This results in a RF of –14 mW/m^2 (2000, S1–S1w), –13 mW/m^2 (2030, S4–S4w), and –26 mW/m^2 (2030, S4s–S4w). It should be noted that the sulphate RFs are only rough estimates, as it is expected that SO_4 forcings show a significant variability with emission site and cloud cover, which is not accounted for in this estimate.

RFs from shipping O_3 and CO_2 as well as the direct sulphate forcings for the different scenarios are summarized in Table 3. We have not evaluated the full impact of ship emissions of NO_x on radiative forcing, since the long-term radiative cooling from CH_4 perturbations has not been quantified (Wild et al., 2001). Also not included are contri-

butions to the RF resulting from the indirect aerosol effect. The indirect aerosol effect is negative (Capaldo et al., 1999) and probably larger than the direct sulphate effects estimated here.

4 Discussion

In the previous section, impacts of ship emissions on NO_2, ozone and sulphate distributions have been presented for present-day and 2030 conditions. In general, the results derived from the ensemble mean comprising ten atmospheric chemistry models agree with previous studies based on single models (Lawrence and Crutzen, 1999; Kasibhatla et al., 2000; Davis et al., 2001; Endresen et al. 2003; Derwent et al., 2005). In this section we discuss the main uncertainties that could impact on results presented in Sect. 3 (Sect. 4.1) and how the results might change in the context of other emission scenarios (Sect. 4.2).

4.1 Uncertainties

4.1.1 Uncertainties in ship emission inventories

Uncertainties in the emission inventory include uncertainties in the vessel traffic densities as well as uncertainties in the emission totals and the species that are considered. Several emission inventories for shipping based on energy statistics have been published in recent years resulting in a total fuel consumption below or around 170 Mt per year (e.g. Corbett and Fischbeck, 1997; Corbett et al., 1999; Olivier et al., 2001; Endresen et al., 2003). For example, Endresen et al. (2003) estimate the international fuel consumption from large cargo and passenger vessels above or equal to 100 GT to be 166 Mt/yr, if an additional 10% for auxiliary engines and 5% for port operations are added to the estimated fuel. However, recent studies which used an activity-based approach and statistical information of the total fleet greater than 100 GT including the

larger military vessels and auxiliary engines (Lloyd's, 2002) suggest a fuel consumption of 289 Mt/yr (Corbett and Köhler, 2003) or 280 Mt/yr (Eyring et al. 2005a) for the year 2001. Ideally, the fuel consumption calculated from energy statistics and with an activity-based approach would be the same. However, there is an ongoing discussion on the baseline value for 2000 fuel consumption. Endresen et al. (2004) questioned the estimated fuel consumption of 289 Mt calculated in the Corbett and Köhler (2003) study, whereas Corbett and Köhler (2004) considered alternative input parameters in their activity-based fuel consumption and emission model and conclude that alternative assumptions in the input parameters could reduce their estimates, but not by more than 14% to 16%. Eyring et al. (2005a) also discussed the different approaches and concluded that any fuel consumption below 220 Mt would lead to unrealistically low average engine hours. The emission totals for NO_x used in this study are around a factor of two lower than those calculated from activity-based approaches.

Vessel traffic densities in the inventory used here are based on EDGAR 3.2 (Olivier et al., 2001). Compared to other data sets such as the Comprehensive Ocean-Atmosphere Data Set (COADS, see http://www.wmo.ch/web/www/ois/ois-home.htm) or the Automated Mutual-assistance Vessel Rescue system (AMVER; Endresen et al., 2003), shipping routes are probably too narrow in this inventory. As pointed out by Lawrence and Crutzen (1999) this could lead to an underestimation of ozone production, as photochemical production is more efficient at lower NO_x concentrations (Liu et al., 1987). However, the emissions are instantaneously diluted into the large model grid boxes (see Table 1) which partly compensates this effect. Over the Baltic emissions in the EDGAR3.2 inventory are higher than in the COADS and AMVER data sets. Note that significant differences between the COADS and AMVER data sets have also been reported (Endresen et al., 2003), as only small subsets of the world-merchant fleet finds input into these data bases.

Assuming that changes in ozone burden scale linearly with increasing NO_x emissions (Sect. 3.2), we conclude that the uncertainty arising from NO_x emission totals in the inventory itself could lead to an underestimation of up to 100% in the simulated

ozone response. We also conclude that due to the inventory used, the process of titration might be overestimated over the Baltic Sea.

The uncertainties in emission inventories discussed above apply also for the future scenarios. In the future, the global distribution of vessel traffic might change. For example, while international trade in north-south direction and within the Southern Hemisphere is likely increasing, the east-west trade on the long-term might reach a level of saturation and hence reduced growth (Eyring et al., 2005b). However, changes in vessel traffic densities are likely to have only small effects on the global scale, though they could regionally be important. For example, with sea ice expected to recede in the Arctic during the 21st century as a result of projected climate warming, Granier et al. (2006) showed that the opening of new shipping routes in the Arctic could lead to an important increase in ozone levels in this remote region.

4.1.2 The role of plume dispersion

Emission totals discussed in Sect. 4.1 are based on specific fuel-oil consumption rates and emission indices measured at the manufacturers' engine test beds (e.g. Eyring et al., 2005a). The emission totals are distributed over the globe with the help of vessel traffic densities derived in various ways and are instantaneously spread onto large inventory grid boxes, usually 1° longitude×1° degree latitude, without accounting for chemical dispersion on the sub-grid scale. Those inventories are used as inputs in emission databases such as EDGAR (Olivier et al., 2001) and global modelling studies. The horizontal resolution in the global models used in this study all have even larger grid sizes of a few hundred kilometres (see Table 1). Therefore, emissions from ships are further instantaneously distributed within the large grid boxes. However, several studies have pointed to the importance of chemical conversion in the near field of ships (Kasibhatla et al., 2000; Davis et al., 2001; Song et al., 2003; von Glasow et al., 2003; Chen et al., 2003). Uncertainties in the modelled ozone changes arising from the neglect of plume chemistry are hard to quantify, in particular because the studies cited above are all based on certain meteorological situations, amount of emissions

ACPD
6, 8553–8604, 2006

released by the ship, and daytime. However, the studies all agree in this respect that the lifetime of NO_x is significantly reduced in the plumes, corresponding to high in-plume NO_x destruction. Chen et al. (2005) used a box model and found that more than 80% of the NO_x loss is due to the reaction of NO_2 with OH and the rest due to PAN formation. Comparing the model output to emission plume measurements they found the largest model biases for HNO_3, likely due to an underestimation of HNO_3 sinks due to particle scavenging. The processes have been shown to be highly dependent on the initial concentration of ship plume NO_x, and in general it has been found that the higher the initial NO_x concentration in the plume, the shorter was the NO_x lifetime (Song et al., 2003). Differences in meteorological situations, time of day of the emissions and emission strength due to different types of the ships make it a challenge to develop a useful parameterisation for global models. To ensure mass conservation, it might also be important to introduce effective emissions which include species that are not primarily emitted, similar to those that have been developed for aviation (Petry et al., 1998). As those parameterisations are not yet available, the model simulations have been run without accounting for sub-grid plume chemistry. However, given that we have used a relatively low total emission estimate (Sect. 4.1) we estimate that the uncertainty due to ship plume processes is less than that in the emissions themselves.

4.1.3 Uncertainties due to different model approaches

Uncertainties in different model approaches presented here and discussed in Sect. 3.1 arise from differences in the main characteristics in the models (see Sect. 2.1). The advantage of this study compared to all previous assessments on ship emissions is that an ensemble of ten models has been used, which makes the results more robust, because the models have performed the same experiments with quite different treatments of chemical and dynamical processes. In summary, the differences in the simulated contributions from shipping to ozone, NO_2, sulphate and RF are smaller than 20%, as revealed by the intermodel standard deviations.

4.2 Results in the context of other emission scenarios

Up to now we have only quantified the impact of ship emissions in 2030 under the assumption that all other emissions vary as projected in the A2 scenario. The A2 scenario is a rather pessimistic scenario, which describes a very heterogeneous world with high population growth. Economic development is primarily regionally oriented and per capita economic growth and technological changes are more fragmented and slower than in other IPCC SRES storylines. NO_x emissions in A2 increase to 179 $Tg(NO_2)\,yr^{-1}$ in 2030. However, if ground based emissions grow less rapidly than under A2, the relative contribution of ship emissions will become more important. The "RAINS Current Legislation Scenario (CLE)" scenario takes into account the current perspectives of individual countries on future economic development and anticipated effects of presently decided emission control legislation in the individual countries and the "Maximum technically Feasible Reduction" (MFR) scenario considers the scope for emission reductions offered by full implementation of the presently available emission control technologies, while maintaining the projected levels of anthropogenic activities. A detailed description of the two scenarios can be found in Dentener et al. (2005). Compared to today's anthropogenic NO_x emissions (91.3 $Tg(NO_2)\,yr^{-1}$ in S1; not including biomass burning), NO_x emissions in the CLE scenario increase to 108 $Tg(NO_2)\,yr^{-1}$ and decrease to 43.0 $Tg(NO_2)\,yr^{-1}$ in the MFR scenario in 2030 (Stevenson et al., 2006, Table 3). Differences in tropospheric ozone burden between 2030 and 2000 for the three scenarios A2, CLE, and MFR have been calculated from an ensemble of 26 models in Stevenson et al. (2006), their Table 6. The simulated inter-scenario ensemble mean changes in ozone burdens between 2030 and 2000 resulted in 53±10 $Tg(O_3)$ in the A2 scenario with ship emissions remaining at 2000 levels (S4–S1), 20±4 $Tg(O_3)$ in the CLE scenario, and –16±4 $Tg(O_3)$ in the MFR scenario. If we add on the 1.75 $Tg(O_3)$ increase in ozone burdens due to ship emission increase under the "Constant Growth Scenario" calculated in this study (see Fig. 7) to the difference in ozone burden between the S4 and the S1 simulation from Stevenson et al. (2006), the global mean relative

ACPD
6, 8553–8604, 2006

EGU

contribution from shipping is around 3% under the A2 scenario. However, under the CLE scenario the relative contribution of ships to ozone burden trends until 2030 increases to around 9%. If land-based emissions fall, as under the MFR scenario, but ship emissions continue to grow, they will significantly counteract the benefits derived from the land-based emissions reductions.

As an example how increases in ship emissions might impact on future trends, Fig. 11 shows differences in near-surface NO_2, ozone and sulphate between the 2030 A2 scenario and 2000 over Europe if ship emissions are zero in 2030 (S4w–S1; left column), remain constant at 2000 levels (S4–S1; middle column), or increase with a constant growth rate of 2.2%/yr (S4s–S1; right column).

If NO_x emissions from shipping fall to zero in 2030, a decrease in near-surface NO_2 concentrations between 2030 and 2000 of up to 2 ppbv over Scandinavia and 0.4 ppbv over the Atlantic can be reached (a reduction of over 50%), whereas central Europe is dominated by increases due to the rise in land NO_x emissions (Fig. 11a). On the other hand, with constant or increasing emissions from shipping (Figs. 11b, c) near-surface NO_2 levels are enhanced over the continent by up to 2 ppbv (>50%), in particular over the coastal regions of the North Sea and the Baltic Sea as well as over the southern part of Great Britain. Only small differences in ozone are simulated under the three different ship emission scenarios (Figs. 11d–f). In a world without ship NO_x emissions in 2030, the positive trend in near-surface ozone will be reduced over most of Europe (Fig. 11d), whereas it will be enhanced in the "Constant Growth Scenario" (Fig. 11f).

The strongest impact of ship emissions to the trends up to 2030 is simulated in the sulphate distributions. A significant decrease in sulphate is simulated in a world without ship emissions in 2030 (Fig. 11g). If ship emissions however remain at today's levels, this negative trend over Central Europe and the United Kingdom is reduced and even changes sign over large areas of the Atlantic and over Scandinavia under the "Constant Growth Scenario" (Fig. 11i). Thus, increasing emissions from shipping would significantly counteract the benefits derived from reducing SO_2 emissions from all other anthropogenic sources under the A2 scenario over the continents in Europe.

ACPD
6, 8553–8604, 2006

EGU

5 Summary and conclusions

In this study we have used an ensemble of ten state-of-the-art global atmospheric chemistry models to assess the impact of NO_x emissions from international shipping on ozone for present-day conditions (year 2000). This multi-model approach accounts for intermodel differences and therefore makes the results more robust compared to previous studies. In addition this study for the first time quantifies the potential impact of ship emissions in the future (year 2030). A subset of four models included the tropospheric sulphur cycle. The ensemble mean of these four models has been applied to investigate the changes in sulphate distributions due to SO_2 emissions from international shipping for present-day conditions and in 2030.

For present-day conditions we find the most pronounced changes in annual mean tropospheric NO_2 and SO_4 columns over the Baltic and the North Sea, and also though smaller over the Atlantic, Gulf of Mexico, and along the main shipping lane from Europe to Asia. Maximum near-surface ozone changes due to NO_x ship emissions are simulated over the North Atlantic in July (~12 ppbv) in agreement with previously reported results (Lawrence and Crutzen, 1999; Endresen et al., 2003). However, in contrast to Endresen et al. (2003), a decrease in ozone in winter is found over large areas in Europe (~3 ppbv) due to titration. Overall NO_x emissions most effectively produce ozone over the remote ocean, where background NO_x levels are small. Evaluation of the models' response to ship emissions with satellite data is still at a preliminary stage. The intercomparison of global models with satellite measurements of tropospheric NO_2 columns is currently limited by the coarse spatial resolution of the models, the uncertainty in the measurements and the difficulty to separate ship emissions from other even stronger emission sources. Unambiguous detection of ship emissions in satellite data is currently only available for the region of the Red Sea and the Indian Ocean (Beirle et al., 2004; Richter et al., 2004), where shipping routes are close to the costal area. Thus, the NO_2 columns in the large grid boxes of the models are strongly influenced or even dominated by land emissions. Reduction in measurement uncertainties

through use of long-term averages and data from more instruments (e.g. OMI and GOME-2) combined with better constraints on land-based sources and higher spatial resolution in the models should facilitate such an intercomparison in the future.

The two 2030 scenarios both specify emissions following the IPCC SRES A2 scenario (Nakicenovic et al., 2000). The first future scenario assumes that ship emissions remain constant at 2000 levels and under this scenario a slightly smaller response in ozone and sulphate changes due to shipping is found compared to the present-day contribution from shipping. This indicates that higher background levels tend to slightly reduce the perturbation from ships. The second emission scenario addresses the question of how NO_x and SO_2 emissions from international shipping might influence atmospheric chemistry in the next three decades if these emissions grow unabated and one assumes a constant annual growth rate of 2.2% between 2000 and 2030 ("Constant Growth Scenario"). The models show future increases in NO_x and ozone burden which scale almost linearly with increases in NO_x emission totals under the same background conditions. Therefore, there is evidence that the ship NO_x effect is only weakly subject to saturation in its current magnitude range, and that saturation cannot be expected to help mitigate the effects of near-future increases. In other words a doubling of NO_x emissions from ships in the future might lead to a doubling in atmospheric ozone burdens due to ship emissions. In addition, increasing emissions from shipping would significantly counteract the benefits derived from reducing SO_2 emissions from all other anthropogenic sources under the A2 scenario over the continents for example in Europe. Under the "Constant Growth Scenario" shipping globally contributes with 3% to increases in ozone burden until 2030 and with 4.5% to increases in sulphate. The results discussed above are calculated under the assumption that all other emissions follow the A2 scenario broadly representing a "pessimistic" future situation. However, if future ground based emissions follow a more stringent scenario, the relative importance of ship emissions becomes larger.

Tropospheric ozone forcings due to ships of 9.8 mW/m^2 in 2000 and 13.6 mW/m^2 in 2030 are simulated by the ensemble mean, with standard deviations of 10–15%.

ACPD
6, 8553–8604, 2006

EGU

Compared to aviation (~20 mW/m^2; Sausen et al., 2005) tropospheric ozone forcings from shipping are of the same order in 2000, despite the much higher NO_x emissions from ships (Eyring et al., 2005a). This can be understood because peak changes in ozone due to shipping occur close to the surface, whereas changes in ozone due to aviation peak in the upper troposphere (Grewe et al., 2002). The net radiative forcing is most sensitive to NO_x emissions at altitudes of about 8–12 km because of longer NO_x and O_3 lifetimes, and colder temperatures compared to the surface (Lacis et al., 1990; Brasseur et al., 1998). Ship NO_x reduces the CH_4 lifetime by 0.13 yr in 2000 and by up to 0.17 yr in 2030, introducing a negative radiative forcing that globally probably outweighs the positive ozone radiative forcing, although it is not specifically quantified here. A rough estimate of RF from shipping CO_2 suggests 26 mW/m^2 in 2000 compared to 23 mW/m^2 from aviation CO_2. The direct effect from SO_2 ship emissions is approximately –14 mW/m^2 in 2000 and decreases to a more negative value of –26 mW/m^2 in 2030 under the "Constant Growth Scenario".

The recent rapid rise in ship emissions may have generated O_3 trends that have hitherto been attributed to increases in hemispheric background, and related to North American or Asian anthropogenic emissions, or to changes in forest fire activities (e.g. observations at Mace Head, Simmonds et al., 2005). For example, Lelieveld et al. (2004) report significant surface ozone trends over the Atlantic Ocean, although not particularly over the North Atlantic, where ships appear to have their largest impact in our study. The large rise in ship emissions and the associated increase in ozone may be compromising measures to reduce O_3 in some regions, e.g. Europe and potentially elsewhere (India, western North America). Of the estimated 0.35 Wm^{-2} radiative forcing since 1750 due to increases in tropospheric ozone, our results indicate that about 3% of this is due to ship NO_x emissions.

This study has also investigated the range of results given by the individual models compared to other uncertainties. Uncertainties in the simulated ozone contributions from ships for the different model approaches revealed by the intermodel standard deviations are found to be significantly smaller than estimated uncertainties stemming

from the ship emission inventory, mainly the ship emission totals, the neglect of ship plume dispersion, and the distribution of the emissions over the globe. This reflects that the simulated net change from ship emissions under otherwise relatively clean conditions in global models is rather similar and shows that the atmospheric models used here are suitable tools to study these effects.

Acknowledgements. Co-ordination of this study was supported by the European Union project ACCENT ("Atmospheric Composition Change: the European NeTwork of excellence". http://www.accent-network.org). The study has also been supported by the Helmholtz-University Young Investigators Group SeaKLIM, which is funded by the German Helmholtz-Gemeinschaft and the Deutsches Zentrum für Luft- und Raumfahrt e.V. (DLR).

References

Beirle, S., Platt, U., von Glasow, R., Wenig, M., and Wagner T.: Estimate of nitrogen oxide emissions from shipping by satellite remote sensing, Geophys. Res. Lett., 31, L18102, doi:10.1029/2004GL020312, 2004.

Bey, I., Jacob, D. J., Yantosca, R. M. et al.: Global modelling of tropospheric chemistry with assimilated meteorology: Model description and evaluation, J. Geophys. Res., 106, 23 073–23 095, 2001.

Brasseur, G., Cox, R., Hauglustaine, D. A., Isaksen, I. S. A., Lelieveld, J., Lister, D., Sausen, R., Schumann, U., Wahner, A., and Wiesen, P.: European scientific assessment of the atmospheric effect of aircraft emissions, Atmos. Environ., 32, 2329–2418, 1998.

Capaldo, K., Corbett, J. J., Kasibhatla, P., Fischbeck, P. S., and S. N., Pandis: Effects of ship emissions on sulfur cycling and radiative climate forcing over the ocean, Nature, 400, 743–746, 1999.

Chen, G., Huey, L. G., Trainer, M., Nicks, D., Corbett, J., Ryerson, T., Parrish, D., Neuman, J. A., Nowak, J., Tanner, D., Holloway, J., Brock, C., Crawford, J., Olson, J. R., Sullivan, A., Weber, R., Schauffler, S., Donnelly, S., Atlas, E., Roberts, J., Flocke, F., Hubler, G., and Fehsenfeld, F.: An investigation of the chemistry of ship emission plumes during ITCT 2002, J. Geophys. Res., 110, D10S90, doi:10.1029/2004JD005236, 2005.

Collins, W. J, Stevenson, D. S., Johnson, C. E., and Derwent, R. G.: Tropospheric ozone in a global-scale three-dimensional Lagrangian model and its response to NOx emission controls, J. Atmos. Chem., 26, 223–274, 1997.
Collins, W. J., Derwent, R. G., Garnier, B., Johnson, C. E., Sanderson, M. G., and Stevenson, D. S.: The effect of stratosphere-troposphere exchange on the future tropospheric ozone trend, J. Geophys. Res., 108(D12), 8528, doi:10.1029/2002JD002617, 2003.
Corbett, J. J. and Fischbeck, P.: Emissions from ships, Science, 278(5339), 823– 824, 1997.
Corbett, J. J., Fischbeck, P. S., and Pandis, S. N.: Global nitrogen and sulfur inventories for oceangoing ships, J. Geophys. Res., 104(3), 3457–3470, 1999.
Corbett, J. J. and Köhler, H. W.: Updated emissions from ocean shipping, J. Geophys. Res., 108, 4650, doi:10.1029/2003JD003751, 2003.
Corbett, J. J. and Köhler, H.W.: Considering alternative input parameters in an activity-based ship fuel consumption and emissions model: Reply to comment by Øyvind Endresen et al. on "Updated emissions from ocean shipping", J. Geophys. Res., 109, D23303, doi:10.1029/2004JD005030, 2004.
Davis, D. D., Grodzinsky, G., Kasibhatla, P., Crawford, J., Chen, G., Liu, S., Bandy, A., Thornton, D., Guan, H., and Sandholm, S.: Impact of ship emissions on marine boundary layer NO_x and SO_2 distributions over the Pacific Basin, Geophys. Res. Lett., 28, 235–238, 2001.
Dentener, F., Peters, W., Krol, M., van Weele, M., Bergamaschi, P., and Lelieveld, J.: Interannual variability and trend of CH_4 lifetime as a measure for OH changes in the 1979–1993 time period, J. Geophys. Res., 108(D15), 4442, doi:10.1029/2002JD002916, 2003.
Dentener, F., Stevenson, D.S., Cofala, J., Mechler, R., Amann, M., Bergamaschi, P., Raes, F., and Derwent, R.G.: Tropospheric methane and ozone in the period 1990-2030: CTM calculations on the role of air pollutant and methane emissions controls, Atmos. Chem. Phys., 5, 1731–1755, 2005.
Dentener, F., Stevenson, D. S., Cofala, J., Mechler, R., Amann, M., Bergamaschi, P., Raes, F., and Derwent, R. G.: The global atmospheric environment for the next generation, Environ. Sci. Technol., 40(11), 3586–3594, 2006a.
Dentener, F., Stevenson, D. S., Ellingsen, K., van Noije, T., Schultz, M., et al.: Nitrogen and sulphur deposition on regional and global scales: A multi-model evaluation, Global Biogeochemical Cycles, in press, 2006b.
Derwent, R. G, Stevenson, D. S., Doherty, R. M., Collins, W. J., Sanderson, M. G., Johnson, C. E., Cofala, J., Mechler, R., Amann, M., and Dentener, F. J.: The contribution from ship

emissions to air quality and acid deposition in Europe, Ambio, 34, 54–59, 2005.
Endresen, Ø., Sørgård , E., Sundet, J. K., Dalsøren, S. B., Isaksen, I. S. A., Berglen, T. F., and Gravir, G.: Emission from international sea transportation and environmental impact, J. Geophys. Res. 108, 4560, doi:10.1029/2002JD002898, 2003.
Endresen, Ø., Sørgård, E., Bakke, J., and Isaksen, I. S. A.: Substantiation of a lower estimate for the bunker inventory: Comment on "Updated emissions from ocean shipping", edited by: Corbett, J. J. and Koehler, H. W., J. Geophys. Res., 109, D23302, doi:10.1029/2004JD004853, 2004.
EPA (Environmental Protection Agency, U.S.A.), SPECIATE 3.2, profiles of total organic compounds and particulate matter, http://www.epa.gov/ttn/chief/software/speciate/index.html, 2002.
Esler, J. G.: An integrated approach to mixing sensitivities in tropospheric chemistry: A basis for the parameterization of subgrid-scale emissions for chemistry transport models, J. Geophys. Res., 108 (D20), 4632, doi:10.1029/2003JD003627, 2003.
Eyring, V., Köhler, H. W., van Aardenne, J., and Lauer, A.: Emissions from international shipping: 1. The last 50 years, J. Geophys. Res., 110, D17305, doi:10.1029/2004JD005619, 2005a.
Eyring, V., Köhler, H. W., Lauer, A., and Lemper, B.: Emissions from international shipping: 2. Impact of future technologies on scenarios until 2050, J. Geophys. Res., 110, D17306, doi:10.1029/2004JD005620, 2005b.
Granier, C., Niemeier, U., Jungclaus, J. H., Emmons, L., Hess, P., Lamarque, J.-F., Walters, S., and Brasseur, G. P.: Ozone pollution from future ship traffic in the Arctic northern passages, Geophys. Res. Lett., 33, L13807, doi:10.1029/2006GL026180, 2006.
Grewe, V., Dameris, M., Fichter, C., and Sausen, R.: Impact of aircraft NOx emissions. Part 1: Interactively coupled climate-chemistry simulations and sensitivities to climate-chemistry feedback, lightning and model resolution, Meteorol. Z., 3, 177–186, 2002.
Hauglustaine, D. A., Hourdin, F., Walters, S., Jourdain, L., Filiberti, M.-A., Larmarque, J.-F., and Holland, E. A.: Interactive chemistry in the Laboratoire de Météorologie Dynamique general circulation model : description and background tropospheric chemistry evaluation, J. Geophys. Res., 109, D04314, doi:10.1029/2003JD003957, 2004.
Haywood, J. M. and K. P. Shine: The effect of anthropogenic sulphate and soot aerosol on the clear sky planetary radiation budget, Geophys. Res. Lett., 22(5), 603–606, 1995.
Isaksen I. S. A., Zerefos, C. S., Kourtidis, K., Meleti, C., Dalsoren, S. B., Sundet, J. K.,

Grini, A., Zanis, P., and Balis, D.: Tropospheric ozone changes at unpolluted and semipolluted regions induced by stratospheric ozone changes, J. Geophys. Res., 110 (2), D02302, doi:10.1029/2004JD004618, 2005.
IMO (International Maritime Organization), IMO Sub-Committee on Bulk Materials, 22nd Session, Agenda Item 7, Ref.code IMO, BCH 22/INF.10, IMO, London, 1992.
IMO (International Maritime Organization), Regulations for the prevention of air pollution from ships and NO_x technical code, ANNEX VI of MARPOL 73/78, London, 1998.
IPCC (Intergovernmental Panel on Climate Change): Climate change 2001: The scientific basis. Contribution of Working Group 1 to the Third Assessment Report, edited by: Houghton, J. T., Cambridge University Press, Cambridge, United Kingdom and New York, NY, USA, 2001.
Kasibhatla, P., Levy II, H., Moxim, W. J., Pandis, S. N., Corbett, J. J., Peterson, M. C., Honrath, R. E., Frost, G. J., Knapp, K., Parrish, D. D., and Ryerson, T. B.: Do emissions from ships have a significant impact on concentration of nitrogen oxides in the marine boundary layer?, Geophys. Res. Lett., 27(15), 2229–2233, 2000.
Labrador, L. J., von Kuhlmann, R., and Lawrence, M. G.: Strong sensitivity of the global mean OH concentration and the troposphere's oxidizing efficiency to the source of NO_x from lightning, Geophys. Res. Lett., 31(6), L06102, doi:10.1029/2003GL019229, 2004.
Lacis, A. A., Wuebbles, D. J., and Logan, J. A.: Radiative forcing of climate by changes in the vertical distribution of ozone, J. Geophys. Res., 95, 9971–9981, 1990.
Langner, J. and Rodhe, H.: A global three-dimensional model of the tropospheric sulphur cycle. J. Atmos. Chem., 13, 225–263, 1991.
Lawrence, M. G. and Crutzen, P. J.: Influence of NO_x emissions from ships on tropospheric photochemistry and climate, Nature, 402, 167–170, 1999.
Lawrence, M. G., Crutzen, P. J., Rasch, P. J., Eaton, B. E., and Mahowald, N. M.: A model for studies of tropospheric photochemistry: Description, global distributions, and evaluation. J. Geophys. Res., 104, 26 245–26 277, 1999.
Lelieveld, J., van Ardenne, J., Fischer, H., de Reus, M., Williams, J., and Winkler, P.: Increasing ozone over the Atlantic Ocean, Science, 304(5676), 1483–1487, 2004.
Lloyd's Maritime Information System (LMIS), The Lloyd's Maritime Database [CD-ROM], Lloyd's Register–Fairplay Ltd., London, 2002.
Olivier, J. G. J. and Berdowski, J. J. M.: Global emissions sources and sinks, in The climate system, edited by: Berdowski, J. J. M., Guicherit, R., and Heij, B. J., Balkema, A. A., Pub-

lishers/Swets & Zeitlinger Publishers, Lisse, The Netherlands, 2001.
Petry, H., Hendricks, J., Mollhoff, M., Lippert, E., Meier, A., Ebel, A., and Sausen R.: Chemical conversion of subsonic aircraft emissions in the dispersing plume: Calculation of effective emission indices, J. Geophys. Res., 103, 5759–5772, 1998.
Rasch, P. J., Mahowald, N. M. and Eaton, B. E.: Representations of transport, convection and the hydrologic cycle in chemical transport models: Implications for the modeling of short lived and soluble species, J. Geophys. Res., 102, 28 127–28 138, 1997.
Richter, A., Eyring, V., Burrows, J. P., Bovensmann, H., Lauer, A., Sierk, B., and Crutzen, P. J.: Satellite measurements of NO_2 from international shipping emissions, Geophys. Res. Lett., 31, L23110, doi:10.1029/2004GL020822, 2004.
Sadourny, R. and Laval, K.: January and July performance of the LMD general circulation model, in: New Perspectives in Climate Modeling, edited by: Berger, A. and Nicolis, C., 173–197, Elsevier, 1984.
Sausen, R. and Schumann, U.: Estimates of the climate response to aircraft CO_2 and NO_x emissions scenarios, Climatic Change, 44, 27–58, 2000.
Sausen, R., Isaksen, I. S. A., Grewe, V., Hauglustaine, D. A., Lee, D. S., Myhre, G., Köhler, M. O., Pitari, G., Schumann, U., Stordal, F., and Zerefos, C.: Aviation radiative forcing in 2000: An update on IPCC (1999), Meteorol. Z., 14, 555–561, 2005.
Scorer, R. S.: Ship trails, Atmos. Environ., 21, 1417–1425, 1987.
Shindell, D. T., Faluvegi, G., Stevenson, D. S., Emmons, L. K., Lamarque, J.-F., Pétron, G., Dentener, F. J., Ellingsen, K., Amann, M., Atherton, C. S., Bergmann, D. J., Bey, I., Butler, T., Cofala, J., Collins, W. J., Derwent, R. G., Doherty, R. M., Drevet, J., Eskes, H. J., Fiore, A. M., Gauss, M., Hauglustaine, D. A., Horowitz, L. W., Isaksen, I. S. A., Krol, M. C., Lawrence, M. G., Montanaro, V., Müller, J.-F., Pitari, G., Prather, M. J., Pyle, J. A., Rast, S., Rodriguez, J. M., Sanderson, M. G., Savage, N. H., Schultz, M. G., Strahan, S. E., Sudo, K., Szopa, S., Unger, N., van Noije, T. P. C., Wild, O., and Zeng, G.: Multi-model simulations of carbon monoxide: Comparison with observations and projected near-future changes, J. Geophys. Res., in press, 2006.
Simmonds, P. G., Manning, A. J., Derwent, R. G., Ciais, P., Ramonet, M., Kazan, V., and Ryall, D.: A burning question. Can recent growth rate anomalies in the greenhouse gases be attributed to large-scale biomass burning events?, Atmos. Environ., 39(14), 2513–2517, 2005.
Song, C. H., Chen, G., Hanna, S. R., Crawford, J., and Davis, D. D.: Dispersion and chem-

ical evolution of ship plumes in the marine boundary layer: Investigation of O_3 /NO_y /HO_x chemistry version, J. Geophys. Res., 108, 4143, doi:10.1029/2002JD002216, 2003.
Stevenson, D. S., Johnson, C. E., Collins, W. J., Derwent, R. G., Shine, K. P., and Edwards, J. M.: Evolution of tropospheric ozone radiative forcing, Geophys. Res. Lett., 25, 3819–3822, 1998.
Stevenson, D. S., Doherty, R. M., Sanderson, M. G., Collins, W. J., Johnson, C. E., and Derwent, R. G.: Radiative forcing from aircraft NO_x emissions: mechanisms and seasonal dependence, J. Geophys. Res., 109, D17307, doi:10.1029/2004JD004759, 2004.
Stevenson, D. S., Dentener, F. J., Schultz, M. G., Ellingsen, K., van Noije, T. P. C., Wild, O., Zeng, G., Amann, M., Atherton, C. S., Bell, N., Bergmann, D. J., Bey, I., Butler, T., Cofala, J., Collins, W. J., Derwent, R. G., Doherty, R. M., Drevet, J., Eskes, H. J., Fiore, A. M., Gauss, M., Hauglustaine, D.A., Horowitz, L.W., Isaksen, I. S. A., Krol, M. C., Lamarque, J.-F., Lawrence, M. G., Montanaro, V., Müller, J.-F., Pitari, G., Prather, M. J., Pyle, J. A., Rast, S., Rodriguez, J. M., Sanderson, M. G., Savage, N. H., Shindell, D. T., Strahan, S. E., Sudo, K., and Szopa, S.: Multimodel ensemble simulations of present-day and near-future tropospheric ozone, J. Geophys. Res., 111, D08301, doi:10.1029/2005JD006338, 2006.
Sudo, K., Takahashi, M., Kurokawa, J., and Akimoto, H.: CHASER: A global chemical model of the troposphere 1. Model description, J. Geophys. Res., 107, 4339, doi:10.1029/2001JD001113, 2002a.
Sudo, K., Takahashi, M., and Akimoto, H.: CHASER: A global chemical model of the troposphere 2. Model results and evaluation, J. Geophys. Res., 107, 4586, doi:10.1029/2001/JD001114, 2002b.
Sudo, K., Takahashi, M., and Akimoto, H.: Future changes in stratosphere-troposphere exchange and their impacts on future tropospheric ozone simulations, Geophys. Res. Lett., 30, 2256, doi:10.1029/2003GL018526, 2003.
Sundet, J. K.: Model Studies with a 3-D Global CTM using ECMWF data. Ph.D. thesis., Dept. of Geophysics, University of Oslo, Norway, 1997.
Times Books: The Times Atlas of the World Comprehensive Edition 9th edn, London, 1992.
van der Werf, G. R., Randerson, J. T., Collatz, G. J., Giglio, L., Kasibhatla, P. S., Arellano Jr., A. F., Olsen, S. C., and Kasischke, E. S.: Continental-scale partitioning of fire emissions during the 1997 to 2001 El Niño/La Niña period, Science, 303, 73–76, 2004.
van Noije, T. P. C., Eskes, H. J., van Weele, M., and van Velthoven, P. F. J.: Implications of the enhanced Brewer-Dobson circulation in European Centre for Medium-Range Weather

Forecasts reanalysis ERA-40 for the stratosphere-troposphere exchange of ozone in global chemistry-transport models, J. Geophys. Res., 109, D19308, doi:10.1029/2004JD004586, 2004.

van Noije, T. P. C., Eskes, H. J., Dentener, F. J., Stevenson, D. S., Ellingsen, K., Schultz, M. G., Wild, O., Amann, M., Atherton, C. S., Bergmann, D. J., Bey, I., Boersma, K. F., Butler, T., Cofala, J., Drevet, J., Fiore, A. M., Gauss, M., Hauglustaine, D. A., Horowitz, L. W., Isaksen, I. S. A., Krol, M. C., Lamarque, J.-F., Lawrence, M. G., Martin, R. V., Montanaro, V., Müller, J.-F., Pitari, G., Prather, M. J., Pyle, J. A., Richter, A., Rodriguez, J. M., Savage, N. H., Strahan, S. E., Sudo, K., Szopa, S., and van Roozendael, M.: Multi-model ensemble simulations of tropospheric NO_2 compared with GOME retrievals for the year 2000, Atmos. Chem. Phys., 6, 2943–2979, 2006.

von Glasow, R., Lawrence, M. G., Sander, R., and Crutzen, P. J.: Modeling the chemical effects of ship exhaust in the cloud-free marine boundary layer, Atmos. Chem. Phys., 3, 233–250, 2003.

von Kuhlmann, R., Lawrence, M. G., Crutzen, P. J., and Rasch, P. J.: A model for studies of tropospheric ozone and non-methane hydrocarbons: Model description and ozone results, J. Geophys. Res., 108(D9), 4294, doi:10.1029/2002JD002893, 2003a.

von Kuhlmann, R., Lawrence, M. G., Crutzen, P. J., and Rasch, P. J.: A model for studies of tropospheric ozone and non-methane hydrocarbons: Model evaluation of ozone-related species, J. Geophys. Res., 108(D23), 4729, doi:10.1029/2002JD003348, 2003b.

Wild, O. and Prather, M. J.: Excitation of the primary tropospheric chemical mode in a global 3-D model, J. Geophys. Res., 105, 24 647–24 660, 2000.

Wild, O. and Prather, M. J.: Global tropospheric ozone modeling: Quantifying errors due to grid resolution, J. Geophys. Res., 111, D11305, doi:10.1029/2005JD006605, 2006.

Wild, O., Prather, M. J., and Akimoto, H.: Indirect long-term global radiative cooling from NO_x emissions, Geophys. Res. Lett., 28(9), 1719–1722, 2001.

Wild, O., Sundet, J. K., Prather, M. J., Isaksen, I. S. A., Akimoto, H., Browell, E. V., and Oltmans, S. J.: CTM Ozone Simulations for Spring 2001 over the Western Pacific: Comparisons with TRACE-P Lidar, ozonesondes and TOMS columns, J. Geophys. Res., 108 (D21), 8826, doi:10.1029/2002JD003283, 2003.

Table 1. Participating models. The models are listed alphabetically by name. The horizontal resolution is given in degrees longitude × latitude.

Model	Institute	Contact author	Resolution (lon/lat) levels, top level	Underlying meteorology	Tropospheric chemistry	Stratospheric chemistry	References
CHASER-CTM	FRCGC / JAMSTEC	K. Sudo	2.8°×2.8° L32 3 hPa	CTM: ECMWF operational analysis data for 2000	53 species 140 reactions, Interactive SO_4 aerosol	O_3 relaxed above 50 hPa to observations	Sudo et al. (2002a, b) Sudo et al. (2003)
FRSGC/ UCI	FRCGC/ JAMSTEC	O. Wild	2.8°×2.8° L37 2 hPa	CTM: ECMWF-IFS pieced-forecast data for 2000	35 species, using ASAD (Carver et al., 1997)	LINOZ (McLinden et al., 2000)	Wild and Prather (2000) Wild et al. (2003)
GMI/ CCM3	NASA Global Modeling Iniative	J. M. Rodriguez S. Strahan	5°×4° L52 0.006 hPa	CTM: NCAR MACCM3	85 species offline aerosol surface area	O_3 influx from SYNOZ: 550 Tg/yr	Rotman et al. (2001) Bey et al. (2001)
GMI/ DAO	NASA Global Modeling Initiative	J. M. Rodriguez S. Strahan	5°×4° L46 0.048 hPa	CTM: GEOS-1-DAS assimilated fields for March 1997–Feb 1998	85 species offline aerosol surface area	O_3 influx from SYNOZ: 550 Tg/yr	Rotman et al. (2001) Bey et al. (2001)
LMDz/ INCA	LSCE	D. Hauglustaine S. Szopa	3.75°×2.5° L19 3 hPa	GCM: nudged to ECMWF ERA-40 reanalysis data for 2000	85 species 303 reactions	Stratospheric O_3 nudged towards climatologies above 380 K	Sadourny and Laval (1984) Hauglustaine et al. (2004)
MATCH-MPIC	Max Planck Institute for Chemistry/NCAR	T. Butler M. Lawrence	5.6°×5.6° L28 2 hPa	CTM: NCEP/NCAR reanalysis data for 2000	60 species 145 reactions	Zonal mean O_3 climatology above 30 hPa; above tropopause: NO_y set to prescribed NO_y/O_3 ratios	von Kuhlmann et al. (2003a, b) Lawrence et al. (1999) Rasch et al. (1997)
STOCHEM-HadAM3	University of Edinburgh	D. Stevenson	5°×5° L9 100 hPa	GCM: HadAM3 vn4.5	70 species 174 reactions SO_x-NO_y-NH_x aerosols; interactive	Prescribed O_3 concentration gradient at 100 hPa	Collins et al. (1997) Stevenson et al. (2004)
STOCHEM-HadGEM	UK Met. Office	M. Sanderson B. Collins	3.75°×2.5° L20 40 km	GCM: HadGEM	70 species 174 reactions SO_x-NO_y-NH_x aerosols; interactive	Relaxed towards SPARC O_3 climatology above tropopause	Collins et al. (1997) Collins et al. (2003)
TM4	KNMI	T. van Noije	3°×2° L25 0.48 hPa	CTM: ECMWF 3-6-h operational forecasts for 2000	37 species (22 transported) 95 reactions SO_x-NOy-NHx aerosols, interactive	O_3 nudged towards climatology above 123 hPa: except 30N–30S, above 60 hPa	Dentener et al. (2003) van Noije et al. (2004)
UIO_CTM2	University of Oslo	K. Ellingsen M. Gauss	2.8°×2.8° L40 10 hPa	CTM: ECMWF-IFS forecast data	58 species	O_3, HNO_3 and NO_x from OsloCTM2 model run with stratospheric chemistry	Sundet (1997) Isaksen et al. (2005)

ACPD
6, 8553–8604, 2006

EGU

Table 2. Specified global annual anthropogenic (not including biomass burning emissions) surface emission totals for each scenario.

Name	Meteorology		Emissions			
			NO_x (Tg N)		SO_x (Tg S)	
			Total	Thereof from Shipping	Total	Thereof from Shipping
S1	2000/ 1995–2004	2000 (EDGAR3.2)	27.80	3.10	54.00	3.88
S1w	2000/ 1995–2004	2000 (EDGAR3.2), but without ship emissions	24.70	0.00	50.12	0.00
S4	2000/ 1995–2004	2030 SRES A2, but with ship emissions of the year 2000	54.60	3.10	100.00	3.88
S4s	2000/ 1995–2004	2030 SRES A2, Traffic A2s; Ship emissions increase with a flat increase of 2.2%/yr compared to the year 2000	57.45	5.95	103.48	7.36
S4w	2000/ 1995–2004	2030 SRES A2, but without ship emissions	51.50	0.00	96.12	0.00

Table 3. Radiative forcings due to shipping in 2000 and 2030.

	O_3, mW/m^2	SO_4(direct), mW/m^2	CO_2 mW/m^2
2000 (S1–S1w)	9.8 ± 2.0	–14	26
2030 (S4–S4w)	7.9 ± 1.4	–13	24
2030 (S4s–S4w)	13.6 ± 2.3	–26	46

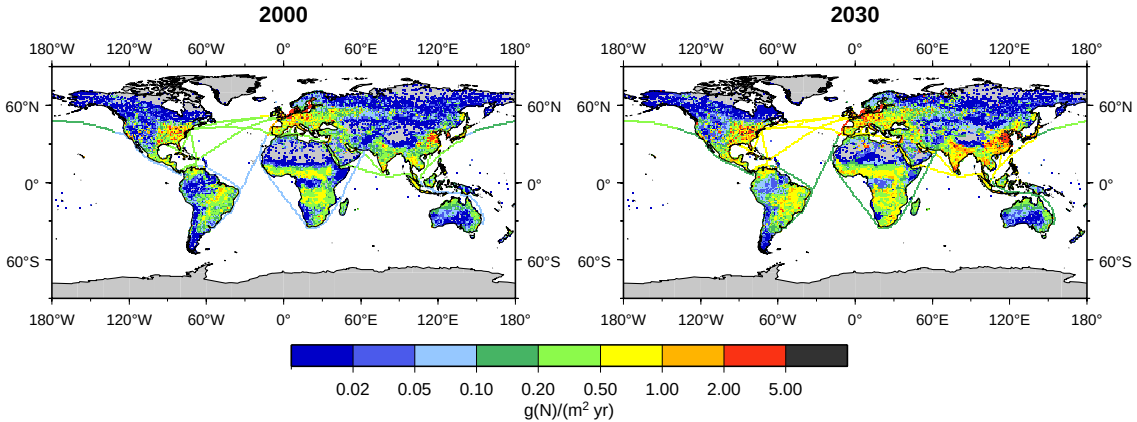

Fig. 1. Annual surface NO_x emissions including industry and power generation, traffic, domestic heating, and biomass burning (average 1997–2002 (van der Werf et al. (2004)) in g(N)/(m^2 yr). The left plot shows the emissions used as input for the model experiment S1 (year 2000, 38.0 Tg(N)/yr total), the right plot the emissions for experiment S4s (year 2030, 67.6 Tg(N)/yr total).

ACPD
6, 8553–8604, 2006

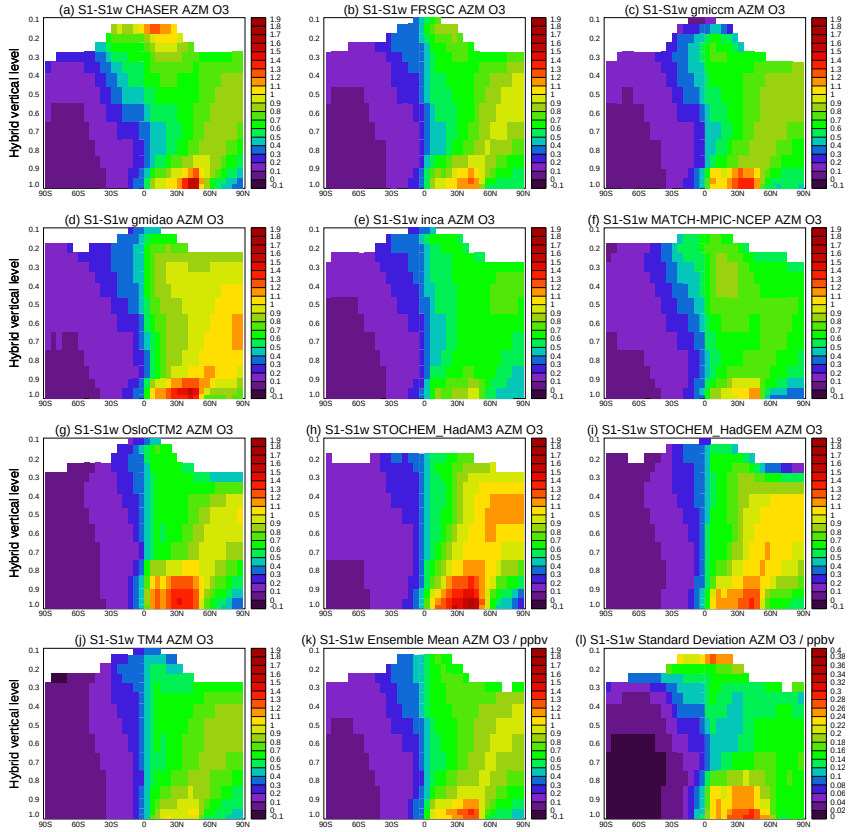

Fig. 2. Modelled zonal annual mean ozone change (ppbv) between case S1 (year 2000) and S1w (year 2000 without ship emissions): **(a)**–**(j)** individual models **(k)** ensemble mean (all 10 models) and **(l)** absolute standard deviations. Individual model results were interpolated to a common grid ($5^{\circ}\times5^{\circ}\times19$ levels) and masked at the chemical tropopause (O_3=150 ppbv).

ACPD
6, 8553–8604, 2006

EGU

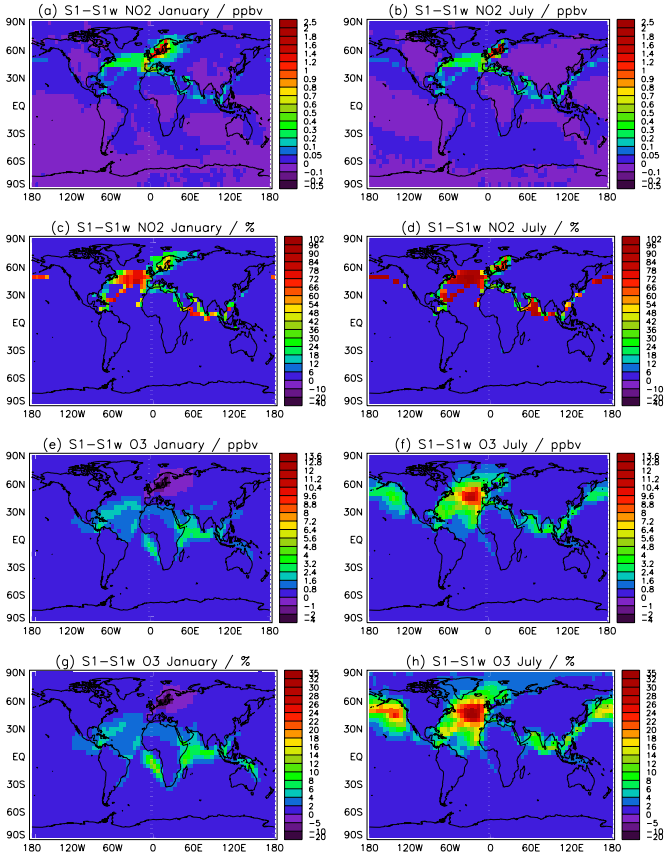

Fig. 3. Modelled ensemble mean near-surface NO_2 and ozone change between case S1 (year 2000) and S1w (year 2000 without ship emissions) in January (left) and July (right). 1st row shows absolute changes in near-surface NO_2 **(a, b)**, 2nd row shows relative changes in near-surface NO_2 **(c, d)**, 3rd row shows absolute changes in near-surface O_3 **(e, f)**, and 4th row shows relative changes in near-surface O_3 **(g, h)**.

ACPD
6, 8553–8604, 2006

EGU

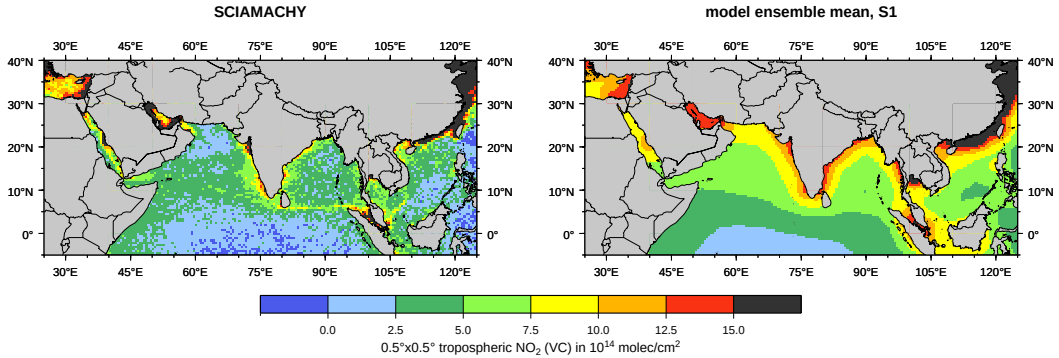

Fig. 4. NO_x signature of shipping in the Indian Ocean (5° S to 40° N and 25° E to 125° E). Left: Tropospheric NO_2 columns derived from SCIAMACHY data from August 2002 to April 2004 (Richter et al., 2004). Right: Ensemble mean NO_2 tropospheric columns at 10:30 local time for 2000. The ensemble mean comprises 8 out of the 10 models. Individual model results and SCIAMACHY data were interpolated to a common grid (0.5°×0.5°).

ACPD
6, 8553–8604, 2006

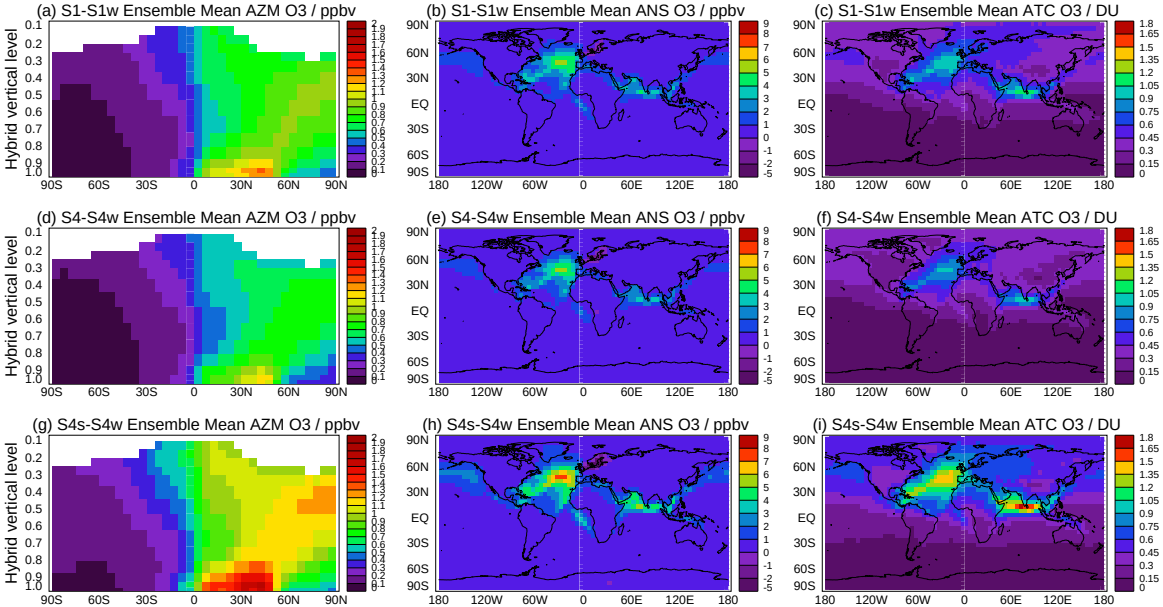

Fig. 5. Modelled ensemble mean ozone change between **(a)**–**(c)** case S1 (year 2000) and S1w (year 2000 without ship emissions), **(d)**–**(f)** case S4 (year 2030) and S4w (year 2030 without ship emissions), and **(g)**–**(i)** case S4s (year 2030) and S4w. Figures 5a, d, and g are zonal mean changes (ppbv), Figs. 5b, e, and h are near-surface ozone changes (ppbv) and Figs. 5c, f, and i are tropospheric ozone column changes (DU).

ACPD
6, 8553–8604, 2006

EGU

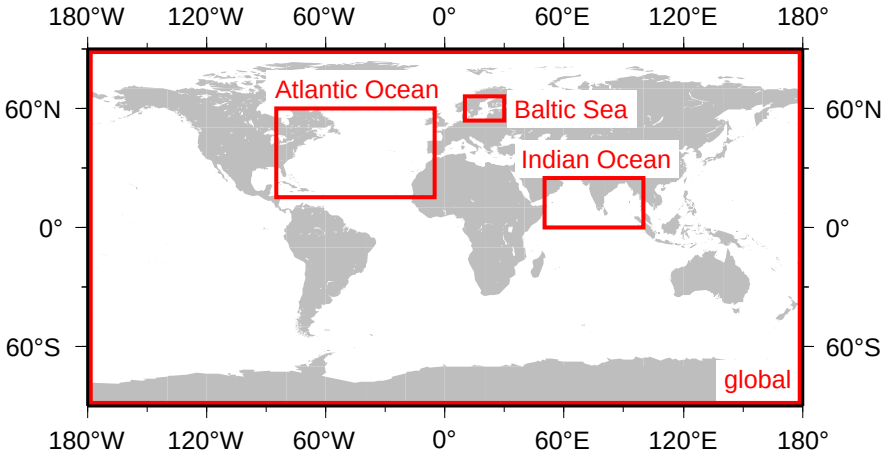

Fig. 6. Regions used in the analysis for Figs. 7 and 8: The Atlantic Ocean (85° W, 15° N–5° W, 60° N), the Baltic Sea (10° E, 54° N–30° E, 66° N), the Indian Ocean (50° E, 0° N–100° E, 25° N) and global.

ACPD
6, 8553–8604, 2006

EGU

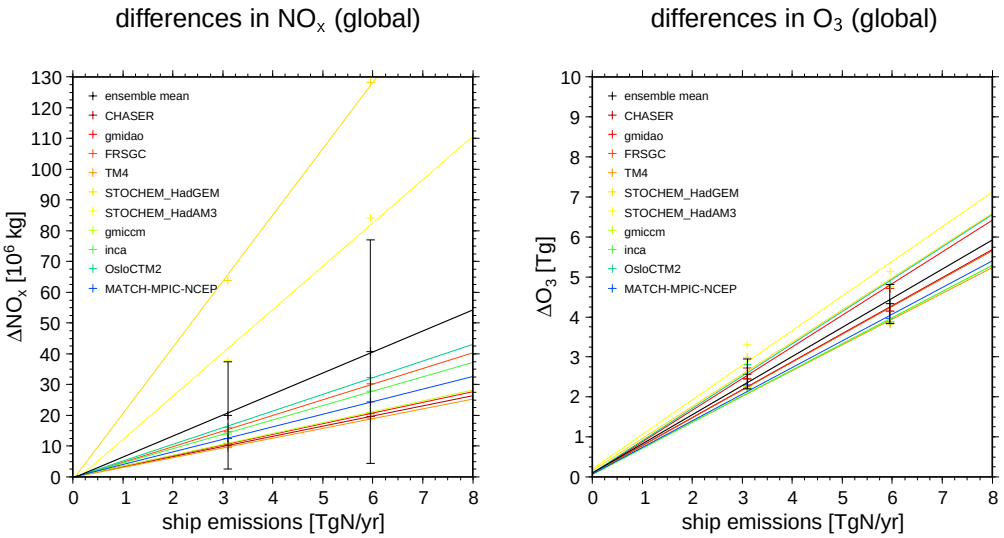

Fig. 7. Global total change in annual mean tropospheric NO_x burden (left) and ozone burden (right) due to ship emissions (S4–S4w and S4s–S4w) in each individual model (coloured lines) and the ensemble mean (black line). Inter-model standard deviations are shown as bars.

ACPD
6, 8553–8604, 2006

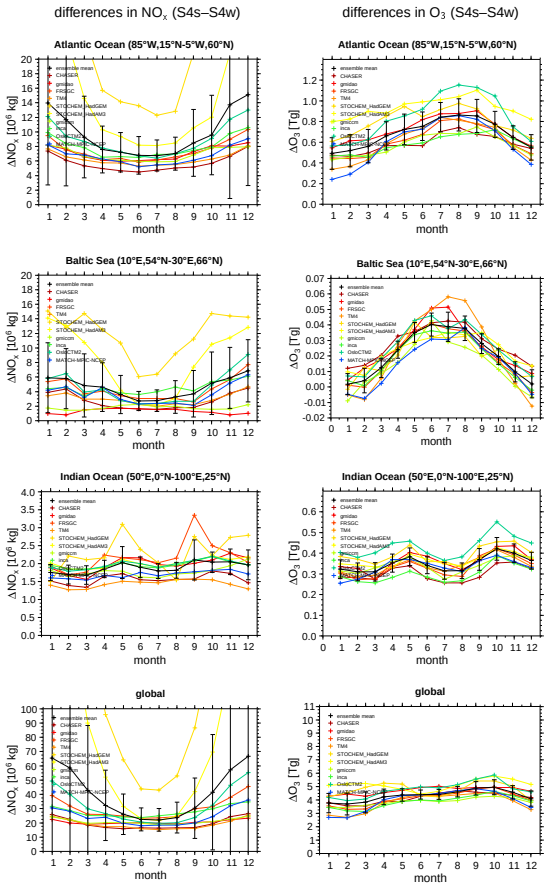

Fig. 8. Seasonal variation in tropospheric NO_x (left) and ozone (right) burden due to shipping versus change in total ship emissions of NO_x for the scenario S4s–S4w in different regions that are shown in Fig. 6: **(a)** Atlantic Ocean, **(b)** Baltic Sea, **(c)** Indian Ocean, and **(d)** global.

ACPD
6, 8553–8604, 2006

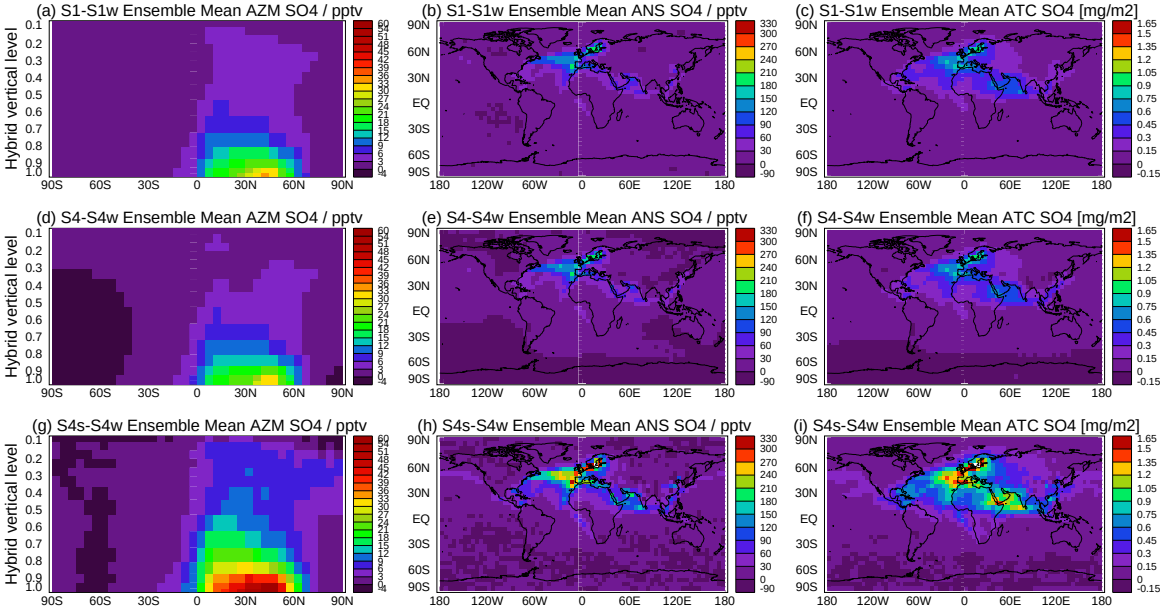

Fig. 9. Modelled ensemble mean tropospheric sulphate changes between **(a)**–**(c)** case S1 (year 2000) and S1w (year 2000 without ship emissions), **(d)**–**(f)** case S4 (year 2030) and S4w (year 2030 without ship emissions), and **(g)**–**(i)** case S4s (year 2030) and S4w. Figures 10a, d, and g are zonal mean changes (pptv), Figs. 10b, e, and h are near-surface sulphate changes (pptv) and Figs. 10c, f, and i are tropospheric sulphate column changes (mg/m^2). Individual model results were interpolated to a common grid (5°×5°×19 levels) and masked at the chemical tropopause (O_3=150 ppbv). The ensemble mean comprises four models.

ACPD
6, 8553–8604, 2006

EGU

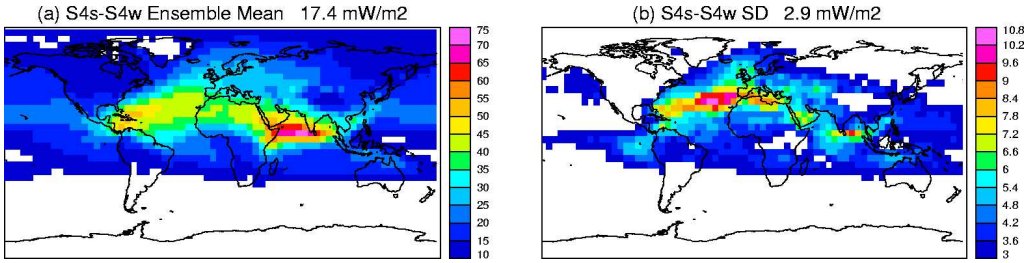

Fig. 10. Ensemble mean for instantaneous tropospheric ozone forcing **(a)** plus standard deviations **(b)** in mW/m^2.

ACPD
6, 8553–8604, 2006

EGU

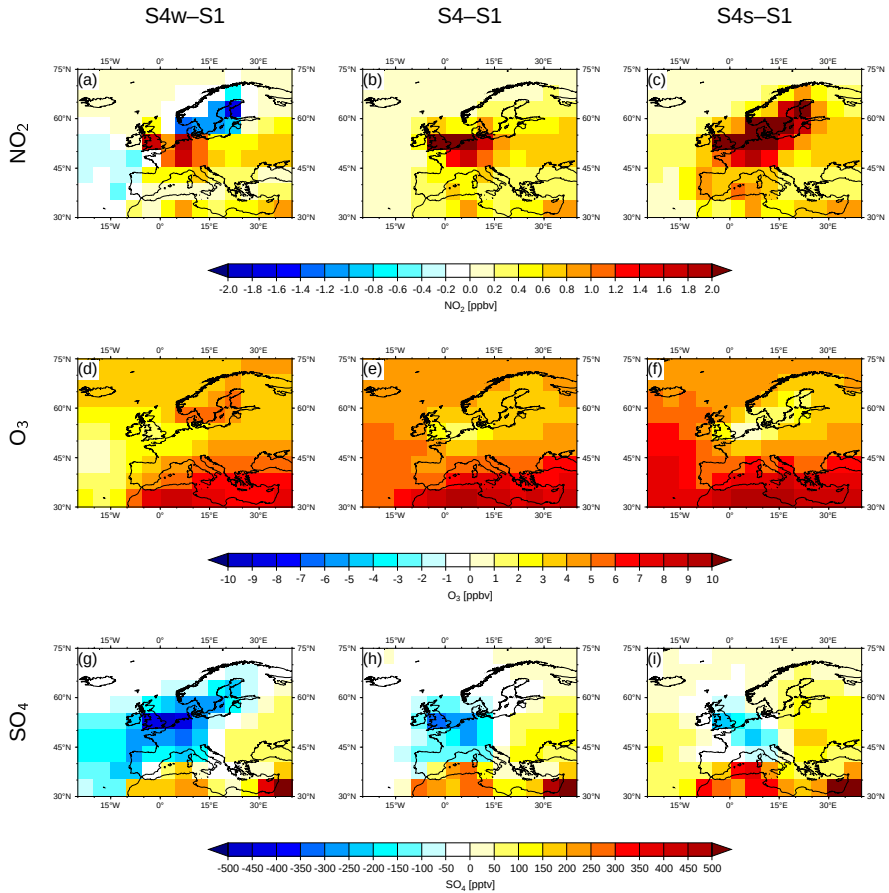

Fig. 11. Changes 2030–2000 over Europe under the IPCC SRES A2 scenario with different assumptions for ship emissions. Left: Changes in a world without ship emissions in 2030; Middle: Changes in a world with ship emissions remaining at 2000 levels; Right: Changes under the "Constant Growth Scenario".